JSE Journal of Systematics and Evolution

doi: 10.1111/jse.12691

Research Article

# Phylogenomics enables biogeographic analysis and a new subtribal classification of Andropogoneae (Poaceae—Panicoideae)

Cassiano A. D. Welker[1†], Michael R. McKain[2†], Matt C. Estep[3], Rémy S. Pasquet[4], Gilson Chipabika[5], Beatrice Pallangyo[6], and Elizabeth A. Kellogg[7*]

[1]Instituto de Biologia, Universidade Federal de Uberlândia, Rua Ceará s/n, Uberlândia, MG 38400-902, Brazil
[2]Department of Biological Sciences, The University of Alabama, 411 Mary Harmon Bryant Hall, Tuscaloosa, AL 35487, USA
[3]Department of Biology, Appalachian State University, Boone, NC 28608, USA
[4]DIADE Research Unit, Université de Montpellier, IRD, Montpellier F-34394, France
[5]Mount Maluku Central Research Station, Zambia Agriculture Research Institute, Chilanga Private Bag 7, Zambia
[6]Biocontrol Program, Kibaha PO Box 30031, Tanzania
[7]Donald Danforth Plant Science Center, 975 North Warson Road, St. Louis, MO 63121, USA
[†]These authors contributed equally to this study.
*Author for correspondence. E-mail: ekellogg@danforthcenter.org
Received 18 June 2020; Accepted 20 September 2020; Article first published online 24 September 2020

**Abstract** The grass tribe Andropogoneae (Poaceae—Panicoideae) includes several important crops such as maize, sugarcane, and sorghum, and dominates the tropical grasslands of the world. We present here a plastome phylogeny of the tribe with the largest sample of genera to date (about 73%), including 65 newly assembled plastomes, together with a broad biogeographic analysis of Andropogoneae. Major relationships found in previous phylogenetic studies were confirmed here, with most nodes having higher resolution and support, including those of the backbone of the tree, which had been a major problem in previous phylogenies of the tribe. Our dated tree suggests that Andropogoneae diverged from Arundinelleae in the Early Miocene, while the "core Andropogoneae" clade originated in the Late Miocene. The tribe originated in East Asia, but intercontinental dispersal has been common, with many independent dispersal events to Africa and the New World. Based on the plastome phylogeny, we propose here a new classification of Andropogoneae as most of its previously accepted subtribes are not monophyletic. Our classification comprises 14 subtribes, 92 genera, and ~1224 species. About 90% of the Andropogoneae species could be assigned to a subtribe, which represents a major step toward clarification of the taxonomy of the tribe. The remaining taxa were placed *incertae sedis* pending additional molecular data. The new subtribes Chrysopogoninae and Rhytachninae are described herein. Our plastome trees also indicate that several Andropogoneae genera are para- or polyphyletic and require additional studies to define their circumscriptions.

**Key words:** dated phylogeny, East Asia, Gramineae, intercontinental dispersal, Miocene, subtribe, whole chloroplast genome.

## 1 Introduction

The tropical grasslands of the world are dominated by a single clade of grasses, the tribe Andropogoneae in subfamily Panicoideae (Clayton & Renvoize, 1986). As of 2017, the tribe comprised about 98 genera and 1202 species (Soreng et al., 2017). Andropogoneae has enormous economic and ecological importance. It includes some of the main plant species for human consumption, such as maize (*Zea mays* L.), sugarcane (*Saccharum officinarum* L.), and sorghum [*Sorghum bicolor* (L.) Moench], as well as important plants used for biofuels, such as *Miscanthus* Andersson and *Saccharum* L. As Estep et al. (2014) noted, "the Andropogoneae feed, and increasingly fuel, the planet." Many ecologically dominant species in grassland formations throughout the world also belong to Andropogoneae, such as species of *Andropogon* L., *Schizachyrium* Nees, and *Themeda* Forssk. (Skendzic et al., 2007; Estep et al., 2014). These wild species provide a rich source of genetic and ecological information that can be extrapolated to the crops; for example, the wild species are hosts for (and presumably therefore tolerate) attack by Lepidopteran stem borers (e.g., Le Ru et al., 2015, 2017), some of which also are serious pests of the Andropogoneae crops maize and sorghum (Sparks, 1979; Day et al., 2017).

Members of Andropogoneae have paired spikelets at each node of the rachis (one sessile or nearly so, the other pedicellate), the spikelets with two florets, and the rachis

usually disarticulating at maturity with the spikelet pair acting as the dispersal unit (Clayton & Renvoize, 1986; Kellogg, 2015). However, the overall form of the inflorescence is extremely variable in the tribe, even within genera or clades (Kellogg, 2015; Arthan et al., 2017). Part of the morphological diversity of inflorescences in Andropogoneae is shown in Fig. 1. Polyploidy and reticulate evolution are very common in Andropogoneae, with a high number of independent allopolyploidization events having occurred over the last 10 million years (Estep et al., 2014). According to Estep et al. (2014), at least a third of all speciation events in the tribe have resulted from allopolyploidy.

Previous molecular phylogenetic studies indicated that Andropogoneae is strongly supported as monophyletic and the genus *Arundinella* Raddi is its sister group (Mathews et al., 2002; Sánchez-Ken & Clark, 2010; Teerawatananon

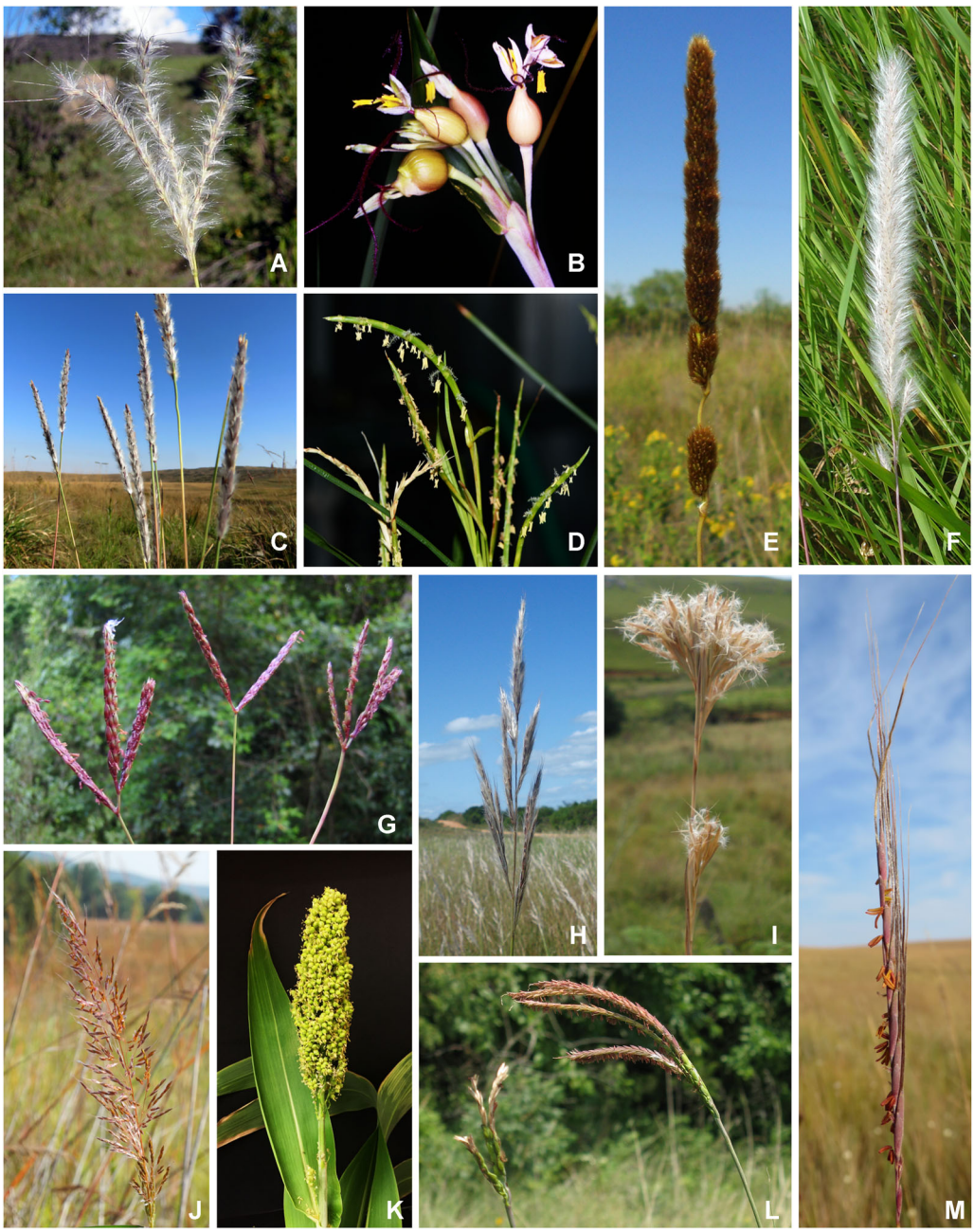


**Fig. 1.** Morphological diversity in Andropogoneae species. **A,** *Andropogon macrothrix* Trin. **B,** *Coix lacryma-jobi* L. **C,** *Elionurus muticus* (Spreng.) Kuntze. **D,** *Hemarthria altissima* (Poir.) Stapf & C.E. Hubb. **E,** *Eriochrysis cayennensis* P. Beauv. **F,** *Imperata tenuis* Hack. **G,** *Ischaemum minus* J. Presl. **H,** *Saccharum intermedium* Welker & Peichoto. **I,** *Schizachyrium condensatum* (Kunth) Nees. **J,** *Sorghastrum nutans* (L.) Nash. **K,** *Sorghum bicolor*. **L,** *Tripsacum dactyloides* (L.) L. **M,** *Trachypogon spicatus* (L. f.) Kuntze. Photo credit: H.M. Longhi-Wagner (A, G); A. Doust (B); C.Z. Fieker (C, M); J. Hodge (D, J); C.A.D. Welker (E, F, H, I); J. Brock (K); E.A. Kellogg (L).

et al., 2011; GPWG II, 2012; Estep et al., 2014). Andropogoneae trees generally have short branches along the backbone of the tree, usually with low support, in contrast to long external branches, suggesting rapid radiation early in the evolution of the tribe (Mathews et al., 2002; Teerawatananon et al., 2011; Estep et al., 2014; Welker et al., 2015). Major results of recent phylogenies of Andropogoneae include the position of the genus *Arthraxon* P. Beauv. as an isolated and early-diverging lineage within the tribe (GPWG II, 2012; Estep et al., 2014; Arthan et al., 2017) and the presence of a "core Andropogoneae" clade which comprises almost half the species of the tribe and includes *Andropogon*, *Bothriochloa* Kuntze, *Hyparrhenia* Andersson ex E. Fourn., *Schizachyrium*, and several other genera (Mathews et al., 2002; Estep et al., 2014; Welker et al., 2016; Arthan et al., 2017). *Zea* L., *Saccharum*, *Miscanthus*, *Sorghum* Moench, and many others are placed outside of the "core Andropogoneae" clade (Estep et al., 2014; Welker et al., 2015, 2016). However, many unresolved questions remain in the phylogeny of Andropogoneae, such as the weakly resolved grade outside the "core Andropogoneae" clade.

Andropogoneae has a pantropical distribution, with only a small number of species extending north or south of ±30° latitude (E. Kellogg, unpublished data). This broad distribution implies extensive dispersal over evolutionary time. However, the biogeographic history of the tribe has received little attention. Hartley (1958) examined the number of species of Andropogoneae as a percentage of the flora in various parts of the world, and found that the flora of Southeast Asia included a higher percentage of Andropogoneae than other regions. He used this pattern to infer that the tribe might have originated in Southeast Asia. Because the percentage of species in Andropogoneae also reflects a lower percentage in other tribes, the measure does not actually capture the abundance of Andropogoneae. Andropogoneae was also investigated in a family-wide study of Poaceae (Bouchenak-Khelladi et al., 2010), but the ancestral region of the tribe was ambiguous, either unable to be assigned or assessed as pantropical (Africa + Eurasia + South America). Other biogeographic investigations are regional (e.g., Zuloaga et al., 2007; New World, containing only 230 species of Andropogoneae), or focus on a small clade (e.g., Guala, 2000; *Agenium* Nees, *Homozeugos* Stapf, and *Trachypogon* Nees). We know of no phylogenetic study that investigated the biogeography of the tribe as a whole.

Both the name of the tribe and its precise delimitation have been the subject of disagreement in the literature. Some authors (e.g., Reveal, 2004; Besnard et al., 2013; Peichoto, 2013; Vorontsova et al., 2013) have claimed that the name Sacchareae should be used, rather than Andropogoneae. However, Welker et al. (2014) put this controversy to rest, showing clearly that Andropogoneae is the correct name. There is also disagreement about whether the *Arundinella* clade (*Arundinella* + *Garnotia* Brongn.) should be recognized as a tribe sister to Andropogoneae (Arundinelleae), or as a subtribe within Andropogoneae (Arundinellinae), with Clayton & Renvoize (1986) and Soreng et al. (2017) choosing the former and Kellogg (2015) choosing the latter. By recognizing Andropogoneae *s.s.*, separate from Arundinelleae, Clayton & Renvoize (1986) and Soreng et al. (2017) implicitly choose the disarticulating rachis as the synapomorphy for the tribe, whereas by recognizing Andropogoneae *s.l.* (including *Arundinella* + *Garnotia*) Kellogg (2015) applies the name to the clade with the synapomorphies of paired spikelets and NADP-ME $C_4$ photosynthesis.

Different subtribal classifications have been proposed for the tribe Andropogoneae (e.g., Clayton & Renvoize, 1986; Kellogg, 2015; Soreng et al., 2017). Based only on morphology, Clayton & Renvoize (1986) divided Andropogoneae into 11 subtribes: Andropogoninae, Anthistiriinae, Chionachninae, Coicinae, Dimeriinae, Germainiinae, Ischaeminae, Rottboelliinae, Saccharinae, Sorghinae, and Tripsacinae. Few of these subtribes, however, have proven to be monophyletic (Mathews et al., 2002; Skendzic et al., 2007; Teerawatananon et al., 2011). According to Kellogg (2015), the reason for this may be that those subtribes are based mainly on inflorescence form, which is a variable character in Andropogoneae even within clades. Based on a molecular phylogenetic approach, Kellogg (2015) recently recognized seven subtribes in Andropogoneae. In her classification, Anthistiriinae was merged into Andropogoninae, and Dimeriinae into Ischaeminae; most genera of Sorghinae were included in Saccharinae; and members of Chionachninae and Coicinae were considered *incertae sedis*. Later, the phylogenetic classification of Soreng et al. (2017) recognized nine subtribes, somewhat similar to those of Kellogg (2015), but accepting Chionachninae, Coicinae, and the monogeneric Arthraxoninae.

This study aimed to (i) reconstruct a dated phylogeny of Andropogoneae with the largest sample so far, based on complete plastome sequences; (ii) perform a biogeographic analysis of the tribe; and (iii) propose a new subtribal classification of Andropogoneae, using all current evidence, and compare it with other recent classifications of the tribe.

## 2 Material and Methods

### 2.1 Taxon sampling

A total of 259 specimens representing 67 genera and 204 species of Andropogoneae *s.s.* was sampled in the plastome phylogenomic and biogeographic analyses (Table S1). Of these genera, 51 (76%) had their respective type species included in the analyses. Eighteen species of 11 genera from the following tribes of Panicoideae were also sampled: Arundinelleae (*Arundinella* and *Garnotia*), Gynerieae (*Gynerium* Willd. ex P. Beauv.), Jansenelleae (*Chandrasekharania* V.J. Nair, V.S. Ramach. & Sreek. and *Jansenella* Bor), Paniceae (*Digitaria* Haller and *Melinis* P. Beauv.), Paspaleae (*Paspalum* L., *Reynaudia* Kunth, and *Steinchisma* Raf.), and Tristachyideae (*Danthoniopsis* Stapf). *Danthoniopsis stocksii* (Boiss.) C.E. Hubb. was used to root the trees, according to GPWG II (2012), Morrone et al. (2012), and Bianconi et al. (2020).

In addition to the new plastomes generated for this study, other plastomes were retrieved from previous studies (e.g., Burke et al., 2016; Arthan et al., 2017; McAllister et al., 2018; Lloyd Evans et al., 2019; Bianconi et al., 2020). Voucher specimens, GenBank accession numbers, and original references (when applicable) of the plastome sequences are listed in Table S1.

**2.2 DNA extraction, plastome sequencing, and assembly**

DNA was isolated using a modified CTAB protocol adapted from Doyle & Doyle (1987) from live and silica dried leaves. DNA quantity was checked using a Nanodrop (Thermo Fisher Scientific, Waltham, MA, USA) and a Qubit 2.0 (Thermo Fisher Scientific). Double-stranded DNA concentrations were used to determine starting material for library preparation. DNA quality controls required the ratio of absorbance at 260/280 nm to be 1.7–2.0 for the sample to be accepted.

DNA samples were sheared using a Covaris S220 (Covaris, Inc., Woburn, MA, USA) with a target size of 300–500 base pairs (bp) at either the University of Missouri DNA Core Facility or the Donald Danforth Plant Science Center. Sequencing libraries were made using the NEBNext Ultra DNA Library Prep Kit for Illumina (New England BioLabs, Ipswich, MA, USA) or the Nextera DNA Library Prep Kit for Illumina (Illumina, San Diego, CA, USA) per the manufacturer's instructions. Libraries were size selected for 300–400 bp insert sizes. Sequencing was conducted at the University of Missouri (UM) DNA Core Facility, the New York University (NYU) School of Medicine Genome Technology Center, the University of Georgia (UGA) Genomics Facility, or the University of Illinois (UI) Roy J. Carver Biotechnology Center. Libraries were sequenced using single-end 100 bp runs on a HiSeq2500 (UM), a paired-end 150 bp rapid run on a HiSeq2500 (NYU), a paired-end 150 bp run on a NextSeq500 (UGA), or a paired-end 250 bp rapid run on a HiSeq2500 (UI).

Plastid genomes were assembled using Fast-Plast (McKain et al., 2017b). Raw reads were trimmed using Trimmomatic v.0.36 (Bolger et al., 2014) with adapter trimming of appropriate adapters (Nextera or NEBNext), a seed mismatch of 1, a palindrome clip threshold of 30, and a simple clip threshold of 10. Reads were further filtered using a sliding window of 10 bp with a minimum average quality score of 20 and a minimum length of 40. Reads were then mapped to a set of Andropogoneae plastid genomes identified from GenBank, which was updated as plastomes were finished, using Bowtie2 v.2.1.0 (Langmead & Salzberg, 2012) under the "very-sensitive-local" parameter set. Mapped reads were assembled using SPAdes v.3.9.0 (Bankevich et al., 2012) with the "only-assembler" option and k-mer sizes of 55, 69, and 87 for sequencing runs with reads of 100 bp, and 55, 87, and 121 for runs with reads larger than 100 bp. Assemblies were filtered based on coverage estimated by SPAdes to remove extremes of coverage in contigs less than 1000 bp. Extremes of coverage are designated as those outside of the range of one standard deviation less than the weighted average coverage to two and a half standard deviations more. This allows for variation in coverage across SPAdes contigs but also removes mitochondrial contamination (much lower coverage from total genomic DNA shotgun reads). The program afin (in Fast-Plast; McKain et al., 2017b) was used to attempt contig fusion and extension using the full, trimmed read set with three iterations. The first iteration consisted of 150 search loops, an initial contig trim of 100 bp, a minimum overlap of 20 bp, a minimum coverage of 2, and a max extension length of 0.75 the max read length for the sample. The second and third iterations consisted of 50 search loops, an initial contig trim of 100 bp, a minimum coverage of 1, and differed with a minimum overlap of 15 and 10 bp, respectively. If the result was a single contig, the assembly sequence_based_ir_id.pl and orientate_plastome_v.2.0.pl scripts were used to identify boundaries of the large single copy (LSC), small single copy (SSC), and inverted repeat (IR) regions of the plastid genomes (McKain et al., 2017b). If an afin run did not result in a full plastome, contigs were assembled manually in Sequencher v.5.3 (Gene Codes Corporation) using *Schizachyrium scoparium* (Michx.) Nash (NC_035032) to scaffold as described in McKain et al. (2016). Gaps were closed through *in silico* plastome walking if possible, but otherwise filled using *N*s. A coverage analysis as implemented in Fast-Plast was done for each plastome to identify regions of low-quality assembly (designated as regions having a coverage less than 15% of the average coverage of the plastome). These were investigated manually and adjusted based on read coverage when necessary.

Plastid genomes were annotated using Verdant (McKain et al., 2017a). Annotations were verified using GenBank validation (https://github.com/mrmckain/Verdant_Utilities/). If any genes were found to be missing from the annotation or seemingly pseudogenized, the assemblies were verified by mapping reads as above and visual inspection in Sequencher. If mapped reads supported an alternative assembly, these changes were made and the plastome reannotated. In all cases, only single-nucleotide indels in homopolymers were found to be problematic. These were identified by estimating read support for both versions of the assembly across the homopolymer with ~10 bp of flanking sequence on each side. If needed, assemblies were adjusted to fit the consensus of the reads. Final annotations are available in GenBank (MT610042–MT610100, MT942627–MT942632).

Plastid genomes were split into LSC, SSC, and IR using a Perl script (https://github.com/mrmckain/Genome_Skimming_Utilities). These regions were aligned individually using MAFFT v.7.313 (Katoh & Standley, 2013) using high-speed default parameters. Once aligned, these regions were concatenated using a Perl script (https://github.com/mrmckain/Genome_Skimming_Utilities). The best base-pair substitution model was determined to be GTR + GAMMA + I using the Aikake Information Criterion (AIC) in ModelTest-NG v.0.1.6 (Darriba et al., 2020). Full plastome alignments were split into regions depicting features (protein-coding gene exons, introns, tRNAs, rRNAs, and intergenic spacers) based on the relative position in the alignment to the annotation of *Schizachyrium scoparium* (NC_035032). These features were used as data blocks in PartitionFinder v.2.1.1 (Stamatakis, 2014; Lanfear et al., 2017) with the branch lengths linked, models set to "all," model selection using AICc (corrected AIC), and searching done with rcluster (Lanfear et al., 2014) to determine the optimal data partitioning scheme for BEAST2 (Bouckaert et al., 2014).

To explore the effect of poorly aligned portions of the sequence on the resulting trees, positions with gaps were identified and removed using Gblocks v.0.91b under the stringent default condition of blocks not allowing any gaps (Talavera & Castresana, 2007).

**2.3 Phylogenomic analyses**

A maximum likelihood (ML) phylogeny was reconstructed using RAxML v.8.2.12 (Stamatakis, 2014) under the GTR +

GAMMA + I evolutionary model with 500 bootstrap replicates for both the original MAFFT alignment and the reduced alignment generated by Gblocks. A time-calibrated ultrametric tree was estimated using BEAST2 v.2.6.1 (Bouckaert et al., 2014). We partitioned the plastid genome features into 119 partitions as identified by the PartitionFinder2 (Lanfear et al., 2017) analysis. The BEAST2 input file was prepared using BEAUTI2 by designating the 119 partitions with linked trees and linked relaxed clock log-normal model estimating the clock rate, and setting the number of discrete rates to equal the number of branches. Each partition received its own site model that was estimated using a GTR model with four gamma rate categories and a starting invariant proportion of 0.05. We allowed for estimation of the substitution rate, shape, invariant proportion, nucleotide frequencies, and all transition/transversion rates in each partition. We designated two nodes as monophyletic to set priors for age estimations. The first node, designated Arundinelleae + Andropogoneae, included all taxa except for *Chandrasekharania keralensis* V.J. Nair, V.S. Ramach. & Sreek., *Jansenella griffithiana* (Müll. Hal.) Bor, *J. neglecta* S.R. Yadav, Chivalkar & Gosavi, *Paspalum malacophyllum* Trin., *P. vaginatum* Sw., *Reynaudia filiformis* (Spreng. ex Schult.) Kunth, *Steinchisma decipiens* (Nees ex Trin.) W.V. Br., *Digitaria glauca* A. Camus, *Melinis minutiflora* P. Beauv., *Gynerium sagittatum* (Aubl.) P. Beauv., and *Danthoniopsis stocksii*. We used a log-normal distribution for this estimate with a mean of 19.1 million years ago (Ma) and a standard deviation of 0.155 to represent the age range estimated by Vicentini et al. (2008). The second node, identified as Paniceae10X + Andropogoneae, included all taxa except for *Digitaria glauca*, *Melinis minutiflora*, *Gynerium sagittatum*, and *Danthoniopsis stocksii*. Again, we used a log-normal distribution with a mean of 24.3 Ma and a standard deviation of 0.131. The XML file for this run is available at FigShare (https://doi.org/10.6084/m9.figshare.12905711). We ran 25 independent runs on the CIPRES cluster (Miller et al., 2010) for up to 100 million generations sampling every 1000. Output trees and log files were then downloaded and combined using shell commands for the trees (script available in FigShare: https://doi.org/10.6084/m9.figshare.12905711) and LogCombiner v.2.6.2 (Bouckaert et al., 2014) with a 20% burnin. Using LogAnalyser v.2.6.2 (Bouckaert et al., 2014), we determined that all variables of the run reached an effective sample size of 200 or greater. We also verified that the independent runs converged by visualizing their trace output using Tracer v.1.7.1 (Rambaut et al., 2018). The final 1999 977 trees were used to produce three maximum clade credibility (MCC) trees using no burnin and the median, mean, and all of the estimated node heights. All MCC trees were equal in topology and estimated ages. We used the MCC tree estimated from all node heights in further analyses. Maximum likelihood bootstrap support (MLBS) and Bayesian posterior probability (BPP) values were recorded on the trees only for those nodes that did not have full support (100% MLBS, 1.0 BPP).

Because Andropogoneae lacks a fossil record, we used the dates estimated by Vicentini et al. (2008), as discussed above. Dating of nodes within the grass family has been the subject of much discussion. As shown by Vicentini et al. (2008) and Christin et al. (2014), dates for grasses differ depending on whether one includes a set of phytoliths from India (Prasad et al., 2005, 2011). While Vicentini et al. (2008) and Christin et al. (2014) included both sets of dates (yielding an "old" estimate that includes the phytoliths and a "young" estimate that excludes them), most studies since then have chosen one set or the other (e.g., Linder et al., 2018; Schubert et al., 2019). Here, we use the "young" estimate because it is generally more consistent with other information about paleoclimate and plant physiology (e.g., vernalization requirements, $C_4$ physiology).

### 2.4 Biogeographic analyses

Geographic distributions of the species were initially compiled from GrassBase (Clayton et al., 2006 onward) and then checked against several floras and taxonomic works (e.g., Clayton, 1969, 1972a; Gould, 1972; de Wet et al., 1981; van Welzen, 1981; Judziewicz, 1990; Davidse et al., 1994; Veldkamp, 1999; van den Heuvel & Veldkamp, 2000; Barkworth et al., 2003; Zuloaga et al., 2003; Wu et al., 2006; Sun et al., 2010; Veldkamp, 2016b; Welker et al., 2019) to exclude nonnative areas. Geographic areas were divided into North America (including northern Mexico), Central America (including southern Mexico and the Caribbean), South America, Europe, Africa, West Asia (west of monsoonal Asia), East Asia, and Oceania.

Historical geographic distributions were inferred using RASP v.4.2 (Yu et al., 2015, 2020). Geographical areas were encoded using the following schema: A = Africa, B = Central America, C = East Asia, D = Europe, E = North America, F = Oceania, G = South America, and H = West Asia. We first removed the distant outgroups (*Digitaria glauca*, *Melinis minutiflora*, *Gynerium sagittatum*, and *Danthoniopsis stocksii*) from the BEAST2 MCC tree (estimated from all node heights) as these taxa represent deep divergence events (>25 Ma) and the sampling between them and Andropogoneae was very sparse. This tree was set as the condensed tree in RASP. We also subsampled evenly from the end of each run to create a set of 1000 posterior trees to be used in the statistical dispersal-vicariance (S-DIVA) analysis (Yu et al., 2015). The S-DIVA (Yu et al., 2015), dispersal-extinction-cladogenesis (DEC) (Ree & Smith, 2008), and Bayesian Binary MCMC (BBM) (Ronquist & Huelsenbeck, 2003; Ali et al., 2012) analyses were run independently in RASP. For all three models, a maximum of eight states (all possible states) were allowed to represent ancestral areas. For the S-DIVA model, we used 1000 posterior trees as described above. For the DEC model, we allowed for all dispersal constraints to remain at the default of 1. For the BBM analysis, we ran the analysis for 5000 000 generations with 10 chains, sampled every 100 generations, discarded the first 100 generations, and kept the temperature at the default of 0.1. We used the estimated (F81) model for state frequencies and a gamma + G model for among-site rate variation.

### 2.5 New classification

The new classification of Andropogoneae proposed in this paper was based primarily on our plastome phylogenomic analysis, with comparisons with published nuclear phylogenies of the tribe (e.g., Estep et al., 2014; Welker et al., 2015, 2016), and taking into account the morphology

and biogeography of the taxa. The new classification is herein compared with other recent classifications of the tribe, especially Clayton & Renvoize (1986), Kellogg (2015), and Soreng et al. (2017).

We searched intensively to find all the names already published at the subtribe rank to identify which would have nomenclatural priority for each clade. To avoid creating spurious names, we propose new subtribal names only for clades that are strongly supported, identified as clades in all methods of analysis, and whose delimitation in our plastome trees is consistent with previous nuclear phylogenetic analyses. We also avoided proposing new monogeneric subtribes unless there was a strong reason to do so. Because of these restrictive criteria, some genera remained *incertae sedis* in our classification due to the lack of molecular data to accurately determine their phylogenetic affinities and inclusion in subtribes.

# 3 Results

### 3.1 Plastid genome structure

Sixty-five plastomes were newly assembled for this study (Table S1). All Andropogoneae species included in the analyses present a highly conserved plastid genome structure typical of Andropogoneae (Arthan et al., 2017; McAllister et al., 2018). Total plastome sequence length ranges from 133 726 (*Andropogon mannii* Hook. f.—MH181237) to 141 407 bp (*Saccharum spontaneum* L.—LS974681), with the LSC region ranging from 79 071 [*Dichanthium annulatum* (Forssk.) Stapf—MH488955] to 83 733 bp (*Sorghum bicolor*—EF115542), the SSC from 12 002 [*Andropogon mohrii* (Hack.) Hack. ex Vasey—MH181216] to 15 488 bp (*Dichanthium annulatum*—MH488955), and the IR from 19 913 (*Andropogon mannii*—MH181237) to 23 429 bp (*Andropogon mohrii*—MH181216). Plastome size (LSC, SSC, IR, and total length) of all specimens included in this study is presented in Table S2.

Not all plastomes were completely assembled and instead had to be scaffolded as described in the Methods. The maximum number of unknown bases (*N*s) added to any of the new assemblies was 252 (out of 140 259 bp), reflecting 0.18% of the assembly. Eight new assemblies had 100 or more *N*s added while 25 had less than 100. The largest number of unique gapped regions was eight (reflecting the assembly being in nine contigs) with 20 assemblies having two or more gaps and 13 having one (Table S2). Coverage of the new plastome assemblies ranged from 11 to 3070X (Table S2).

### 3.2 Maximum likelihood phylogeny

The ML phylogeny is well-supported throughout, with most nodes having full support (100% MLBS). Major relationships are similar to, but often better resolved than, those found in previous studies.

Beginning with Fig. 2A and working up the tree, the clade of *Arundinella* + *Garnotia* is sister to the Andropogoneae *s.s.* clade, with *Thelepogon* Roth + *Lasiurus* Boiss., *Arthraxon*, and *Zea* + *Tripsacum* L. as successive sisters. *Chionachne* R. Br. and *Polytoca* R. Br. form a clade that is sister to the clade formed by the awnless genera *Vossia* Wall. & Griff., *Oxyrhachis* Pilg., *Rhytachne* Desv. ex Ham., *Loxodera* Launert, and *Urelytrum* Hack., but MLBS for their sister relationship is only 76%, relatively weak support in the context of the rest of the tree. The genus *Chrysopogon* Trin. is monophyletic, and sister to a clade of *Eriochrysis* P. Beauv. and *Parahyparrhenia* A. Camus plus two other species assigned to different genera (*Andropogon* and *Eulalia* Kunth). *Microstegium* Nees, *Sehima* Forssk., and *Kerriochloa* C.E. Hubb. form a clade, but its position as sister to the remaining Andropogoneae is weakly supported (60% MLBS). The position of *Elionurus* Humb. & Bonpl. ex Willd. relative to other clades is also ambiguous (Fig. 2A). *Tripidium* H. Scholz is sister to *Coix* L. plus *Rottboellia cochinchinensis* (Lour.) Clayton, and the awnless genera *Thyrsia* Stapf, *Mnesithea* Kunth, *Eremochloa* Buse, *Glyphochloa* Clayton, *Hackelochloa* Kuntze, and *Hemarthria* R. Br. form a clade. However, the relationship of the awnless genera to *Tripidium* + *Coix* clade receives scant support (46% MLBS).

Figure 2B shows a clade of *Eulaliopsis* Honda, *Andropterum* Stapf, *Ischaemum* L., and *Dimeria* R. Br. sister to the remaining species of the tribe. *Eulalia aurea* (Bory) Kunth, *Polytrias* Hack., *Apluda* L., *Homozeugos*, *Trachypogon*, and *Sorghastrum* Nash also form a clade that is sister to a large clade that contains *Germainia* Balansa & Poitr., *Sorghum*, and *Saccharum*, among other genera. Their sister relationship, however, is only moderately supported (79% MLBS). That large clade includes three well-supported internal clades, with the *Germainia* clade sister to the others. The *Germainia* clade also includes *Imperata* Cirillo and *Pogonatherum* P. Beauv., while the *Sorghum* clade also comprises *Cleistachne* Benth., *Sarga* Ewart, and *Lasiorhachis* (Hack.) Stapf. The *Saccharum* clade also includes *Pseudosorghum* A. Camus, *Miscanthus*, and one species of *Eulalia* (Fig. 2B).

*Jardinea congoensis* (Hack.) Franch. is sister to a large well-supported clade that has been called the "core Andropogoneae" by other authors (e.g., Mathews et al., 2002; Estep et al., 2014; Welker et al., 2016; Arthan et al., 2017). Here, the "core Andropogoneae" is divided into two well-supported internal clades. The first includes species of *Heteropogon* Pers., *Cymbopogon* Spreng., *Themeda*, *Iseilema* Andersson, and the well-supported group of *Bothriochloa*, *Capillipedium* Stapf, and *Dichanthium* Willemet (the "BCD" clade of Estep et al., 2014) plus *Euclasta* Franch. (Fig. 2B). The second internal clade of the "core Andropogoneae" includes *Andropogon*, *Schizachyrium*, *Hyparrhenia*, and *Anadelphia* Hack., plus the mono- or oligotypic genera *Diectomis* Kunth, *Diheteropogon* (Hack.) Stapf, *Elymandra* Stapf, *Exotheca* Andersson, *Hyperthelia* Clayton, and *Monocymbium* Stapf (the "DASH" clade of McAllister et al., 2018) (Fig. 2C).

The ML tree suggests that a number of genera are para- or polyphyletic, assuming that the history of the plastome reflects organismal relationships. These include *Andropogon*, *Schizachyrium*, *Elymandra*, *Hyparrhenia*, the genera of the "BCD" clade, *Heteropogon*, *Cymbopogon*, *Miscanthus*, *Saccharum*, *Eulalia*, *Mnesithea*, *Tripidium*, and *Loxodera* (Fig. 2). Several species originally assigned to *Andropogon* appear in unexpected positions in the tree (e.g., *A. brachystachyus* Chapm., *A. burmanicus* Bor, *A. crossotos* Cope), as well as one species of *Schizachyrium* [*S. delavayi* (Hack.) Bor]. For a few of these, we have been able to validate the position by including a second accession (Fig. 2). The placement of those represented by a single accession should be considered provisional until verified by additional accessions.

Fifty species in this phylogeny are represented by more than one accession. In all cases, the two or three accessions fall into the expected generic clade, and in most cases, the multiple accessions are sisters or form a single clade, giving some confidence in the placement of the species. However, in 16 species, the two accessions are not sisters (Fig. 2).

Analyses of the alignment with gapped positions removed did not materially change the tree. Twenty-six nodes in the gapped trees had bootstrap support below 70%, indicated by daggers in Figs. 2A-2C, most of which also received less than full support in the ML or Bayesian analyses. While the analysis without gaps produced some topologies slightly different from those from the full alignment, these alternative topologies were not strongly supported and none affected the monophyly or composition of the subtribes.

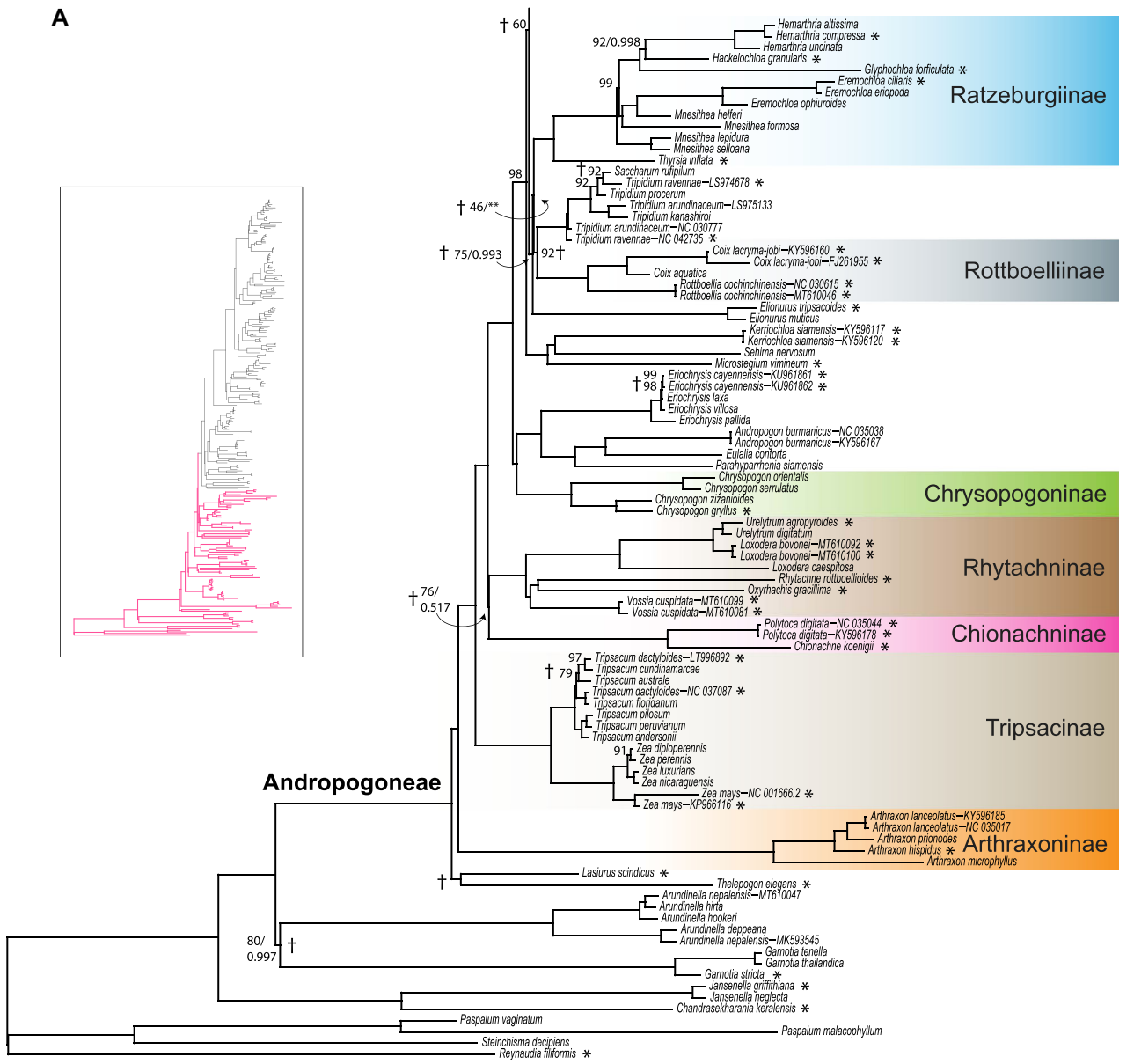


**Fig. 2.** Maximum likelihood tree of Andropogoneae plus select members of Arundinelleae, Jansenelleae, and Paspaleae based on complete plastome sequences. Additional outgroups from Paniceae and other panicoid tribes were included to verify the root of the Andropogoneae but are not shown here. The type species of the genera are marked with an asterisk (*) and the subtribes accepted in this paper are labeled. Maximum likelihood bootstrap values and Bayesian posterior probabilities are 100% and 1.0, respectively, except where indicated (MLBS/BPP). Nodes that differ between the ML and Bayesian trees are indicated by two asterisks (**) after the MLBS value. Nodes that receive less than 70% MLBS support in trees from data with gapped sites removed are marked by a dagger (†). **A**–**C**, subsets of the tree. Inset shows the entire tree, with the relevant subsection highlighted in red.

### 3.3 Dated phylogeny

The topology and estimated divergence times across our three MCC trees were minimally different, with only the divergence times varying insignificantly. The topology of the ultrametric Bayesian phylogeny produced by BEAST2 (Fig. 3) is largely similar to the ML tree (Fig. 2), with most nodes also having full support (1.0 BPP). Nodes with moderate or low support in the ML tree generally also receive scant support in the Bayesian tree, such as the node that indicates the sister relationship of the *Chionachne* and *Rhytachne* clades (76% MLBS, 0.517 BPP).

One major difference between the ML and the Bayesian trees is the position of the genus *Elionurus*. While the genus is weakly supported (0.653 BPP) in the Bayesian tree as sister to the clade formed by the awnless genera *Thyrsia*, *Mnesithea*, *Eremochloa*, *Glyphochloa*, *Hackelochloa*, and *Hemarthria* (Fig. 3A), it is sister to a clade formed by those genera plus *Rottboellia cochinchinensis*, *Coix*, and *Tripidium*

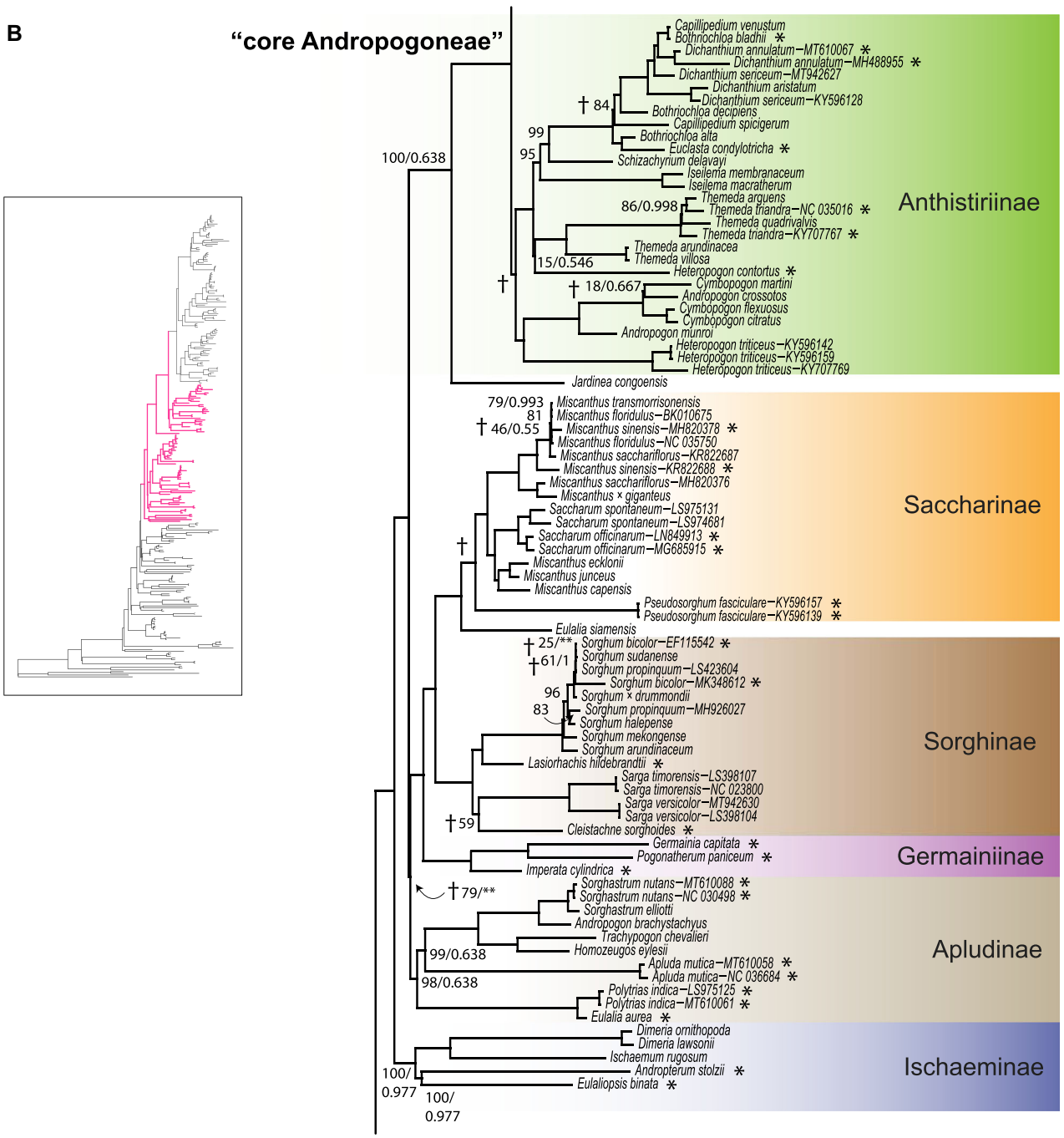


**Fig. 2.** Continued

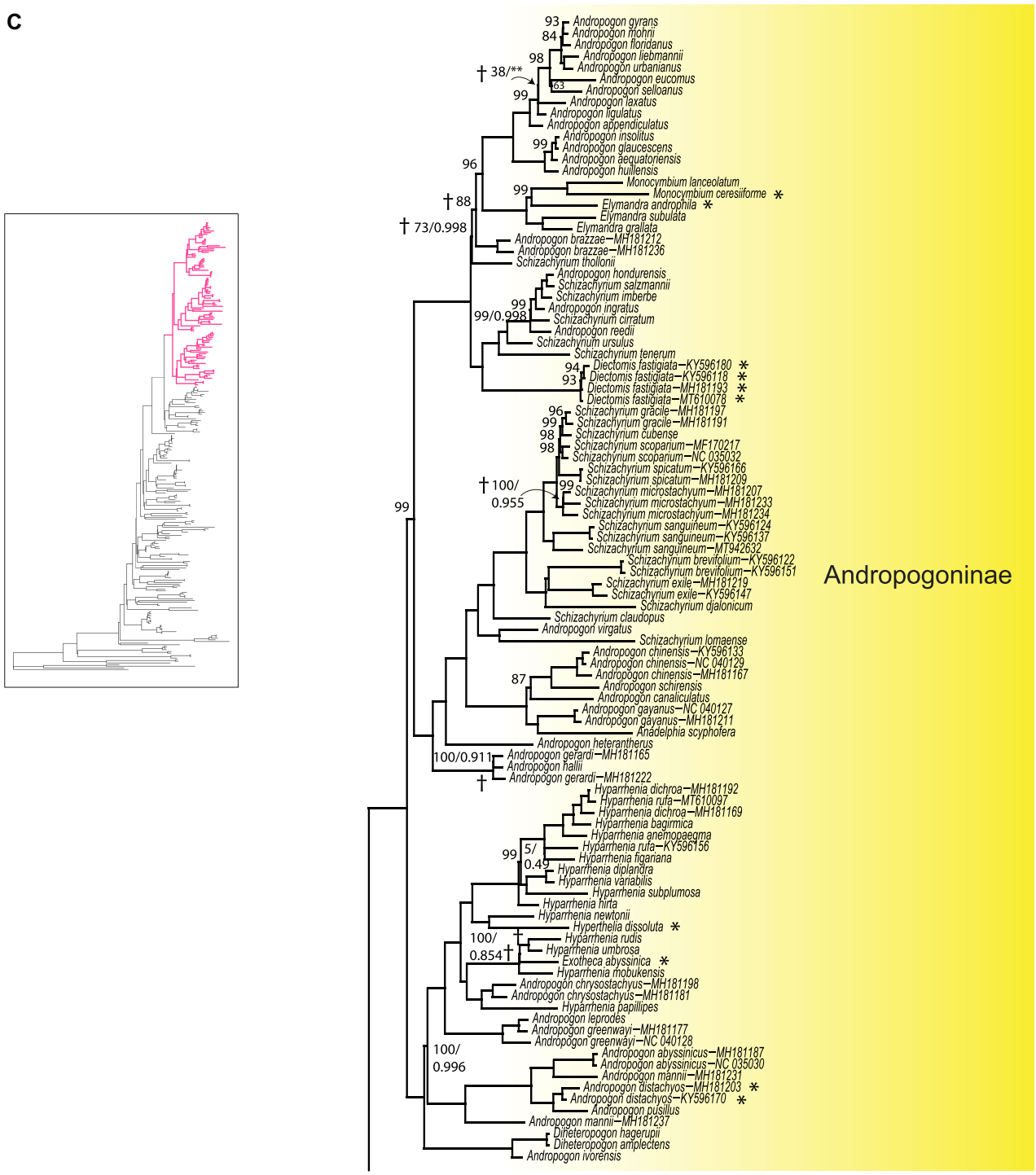


**Fig. 2.** Continued

with scant support (46% MLBS) in the ML tree (Fig. 2A). The other major difference between the trees reflects the position of the clade that includes *Eulalia aurea*, *Polytrias*, *Apluda*, *Homozeugos*, *Trachypogon*, and *Sorghastrum*. This clade is strongly supported in the ML tree (98% MLBS) but receives scant support in the Bayesian tree (0.638 BPP). Additionally, while it is sister to the large clade that includes *Germainia*, *Sorghum*, and *Saccharum* with moderate support (79% MLBS) in the ML tree (Fig. 2B), it is sister to the "core Andropogoneae" clade plus *Jardinea* Steud. with scant support (0.638 BPP) in the Bayesian tree (Fig. 3B). Other differences include the positions of some species within the

genera *Sorghum* and *Andropogon*. In all cases, these differences are associated with very short, and likely difficult to resolve, branches.

The dated phylogeny suggests that Andropogoneae diverged from Arundinelleae at about 17.50 Ma (95% highest posterior density [HPD]: 13.92–21.08 Ma), with the crown Andropogoneae taxa diverging at about 13.89 Ma (95% HPD: 9.89–17.97 Ma) (Fig. 3). The "core Andropogoneae" clade originated at 7.84 Ma (95% HPD: 5.79–9.95 Ma), close to the origin of the "DASH" clade (7.24 Ma; 95% HPD: 5.33–9.13). Crown node ages and 95% HPD values for main clades and subtribes of Andropogoneae accepted in this paper (see the proposed classification below) are presented in Table 1.

### 3.4 Biogeography

All models suggest that dispersal played a prominent role in shaping the biogeographical history of the Andropogoneae, with an estimated 246 (S-DIVA), 291 (DEC), and 373 (BBM)

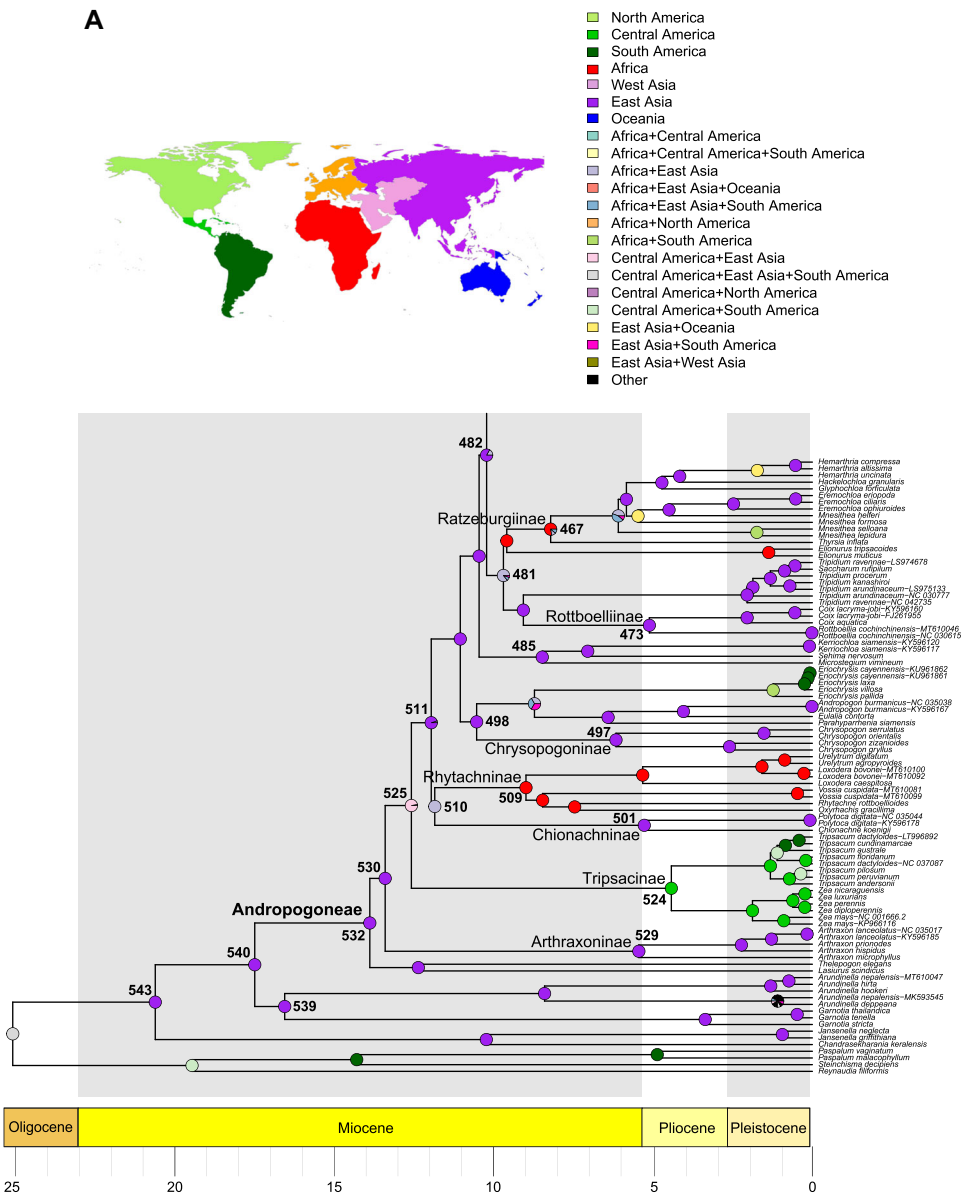


**Fig. 3.** Chronogram of Andropogoneae plus select members of Arundinelleae, Jansenelleae, and Paspaleae based on complete plastome sequences, with ancestral areas estimated using statistical dispersal-vicariance (S-DIVA) analysis. Pie charts indicate ancestral area frequencies with areas and corresponding colors in the legend. Ancestral areas with a frequency of less than 25% present in at least one node are colored black and labeled "Other". A world map with corresponding color codes for single area states depicts our characterization for these regions. RASP node numbers are indicated for subtribes and other nodes discussed in the text. Subtribes are labeled. **A**–**C**, subsets of the chronogram.

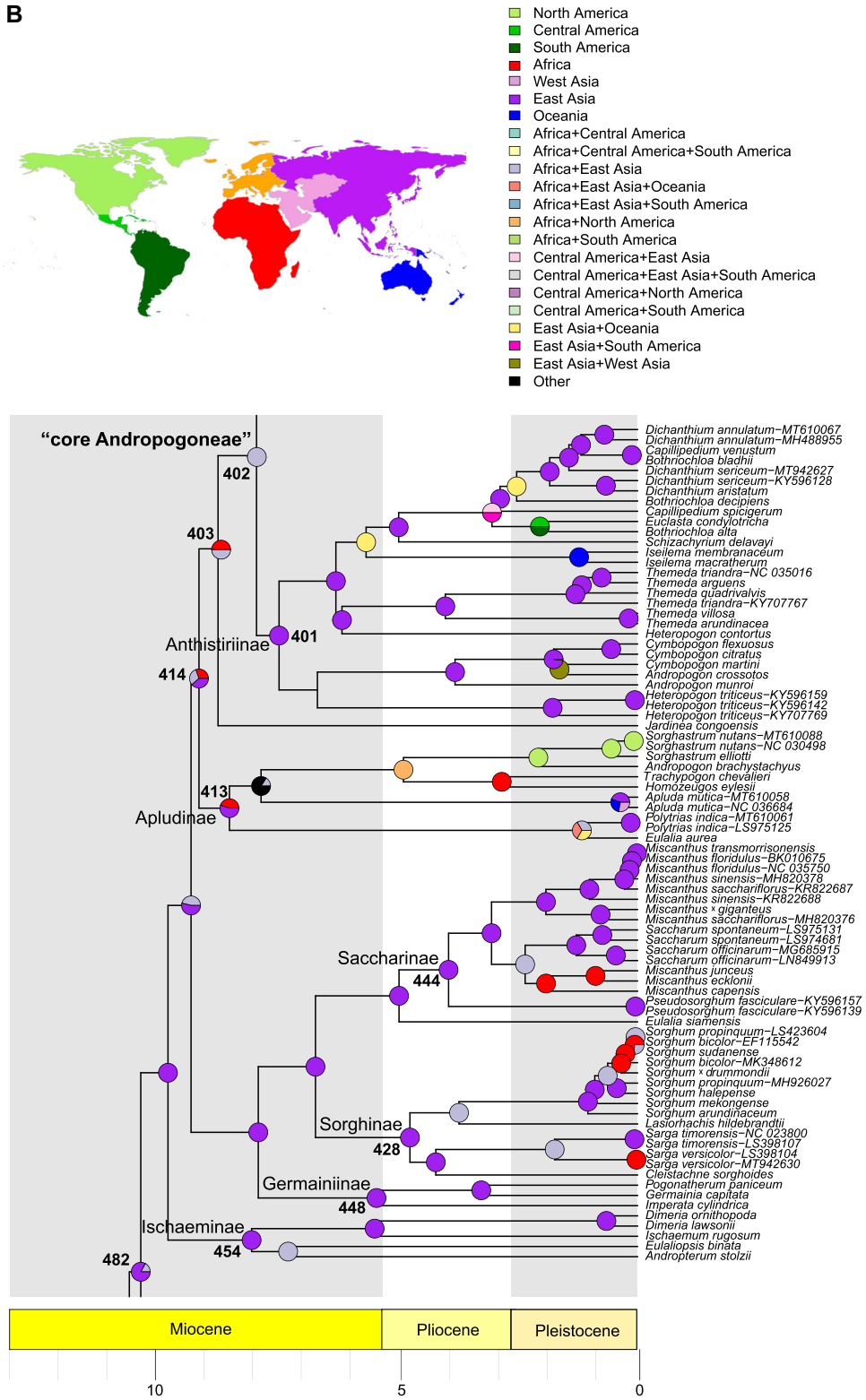


**Fig. 3.** Continued

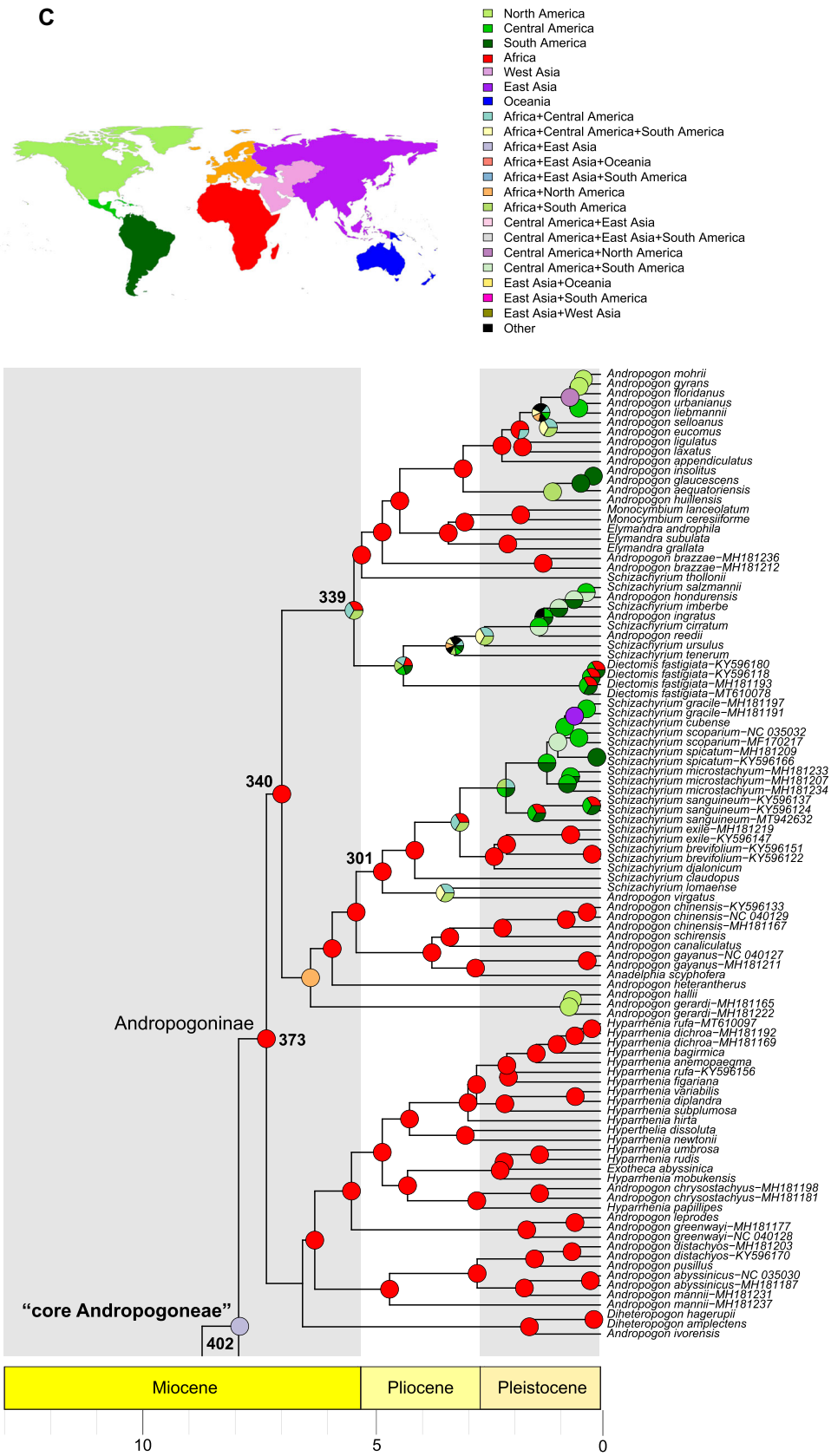


**Fig. 3.** Continued

**Table 1** Crown node age and 95% highest posterior density (HPD) values for main clades and subtribes of Andropogoneae. All values are shown in million years ago (Ma)

| Taxonomic group | Age | Lower 95% HPD | Upper 95% HPD |
|---|---|---|---|
| Jansenelleae-Arundinelleae-Andropogoneae | 20.62 | 16.49 | 25.00 |
| Arundinelleae-Andropogoneae | 17.50 | 13.92 | 21.08 |
| Andropogoneae | 13.89 | 9.89 | 17.97 |
| Arthraxoninae | 5.44 | 2.79 | 8.01 |
| Tripsacinae | 4.42 | 2.05 | 7.77 |
| Chionachninae | 5.27 | 2.10 | 8.37 |
| Rhytachninae | 8.99 | 6.00 | 11.99 |
| Chrysopogoninae | 6.16 | 2.00 | 10.53 |
| Rottboelliinae | 5.11 | 2.92 | 7.65 |
| Ratzeburgiinae | 8.21 | 5.61 | 10.88 |
| Ischaeminae | 7.94 | 5.72 | 10.29 |
| Germainiinae | 5.37 | 3.47 | 7.54 |
| Sorghinae | 4.68 | 5.48 | 10.21 |
| Saccharinae | 3.89 | 2.65 | 6.51 |
| Apludinae | 8.40 | 6.93 | 10.80 |
| "core Andropogoneae" | 7.84 | 5.79 | 9.95 |
| Anthistiriinae | 7.38 | 5.20 | 9.32 |
| Andropogoninae | 7.24 | 5.33 | 9.13 |

unique events across the analyses for the most likely scenario at a given node. In comparison, a total of 35 (S-DIVA), 25 (DEC), and 36 (BBM) vicariance events were estimated for the group. Most of these events have occurred within the last 5 Ma across all analyses. The ancestral range of the Andropogoneae crown-group node was estimated to be East Asia using the models S-DIVA (frequency [freq.] = 100%) and DEC (freq. = 100%). Using the BBM model, it was estimated to be East Asia + Africa (freq. = 74.88%) (Figs. 3A, S1, S2; Table 2). From East Asia, there were 116.67 (S-DIVA), 97.58 (DEC), and 57.17 (BBM) estimated dispersals based on all possible scenarios at a given node (Table S3). The region with the second most dispersals was Africa with 53.17 (S-DIVA), 43.33 (DEC), and 46.83 (BBM) events estimated to have originated from the continent. Few dispersal events originated in Europe and West Asia. There is also limited evidence of dispersal from Oceania except to Africa and West Asia, and those only under the BBM model (Table S3). Given a large number of dispersal events, we discuss here only a few that seem to be most important for interpreting the current distribution of the group. The ancestral areas with frequencies for all subtribes of Andropogoneae are presented in Table 2.

Andropogoneae likely moved from East Asia into Africa one (BBM analysis) to six (S-DIVA and DEC analyses) times during the Miocene: once each for (i) Rhytachninae, (ii) an ancestor of Chrysopogoninae + *Eriochrysis* + *Parahyparrhenia*, (iii) the clade of *Microstegium, Sehima,* and *Kerriochloa,* (iv) Rottboelliinae + *Tripidium,* (v) Ratzeburgiinae, and (vi) sometime before the diversification of Apludinae and the "core Andropogoneae" (Figs. 3, S1, S2).

S-DIVA estimates dispersal from East Asia to Africa at node 511 (probability [*P*] = 0.95) followed by a vicariance event at node 510 (*P* = 1.0) splitting the lineage into Rhytachninae, predominantly African (freq. = 100%), and Chionachinae, East Asian (freq. = 100%) (Fig. 3A). In contrast, DEC places a dispersal event from East Asia to Africa at node 510 (*P* = 0.5445) followed by another dispersal in Africa at node 509 (*P* = 0.4347) (Fig. S1). The DEC analysis estimates the ancestral area of the Rhytachninae crown group to be either Africa + East Asia (freq. = 68.5%) or Africa (freq. = 31.5%) (Fig. S1; Table 2). The BBM analysis estimates dispersal from East Asia to Africa around the divergence of Andropogoneae and Arundinelleae (node 540, *P* = 0.4380), creating a range that spans both Africa and East Asia throughout much of the deep history of the tribe (backbone of the tree). At node 510 (*P* = 0.3943), BBM estimates a dispersal event from this African–East Asian range into a portion of East Asia, giving rise to Chionachinae (freq. = 95.79%). Node 509 sees a similar event dispersing into a portion of Africa (*P* = 0.3559), leading to Rhytachninae (ancestral area: Africa + East Asia; freq. = 61.1%) (Fig. S2; Table 2).

For the clade of Chrysopogoninae plus *Eriochrysis* and *Parahyparrhenia*, S-DIVA estimates dispersal from East Asia (freq. = 100%) to Africa and South America (node 498; *P* = 0.3333) (Fig. 3A). DEC also suggests dispersal from East Asia (freq. = 100%) to Africa and South America (*P* = 0.2276), though after the divergence of the *Eriochrysis-Parahyparrhenia* lineage from the Chrysopogoninae (node 494) (Fig. S1). BBM suggests dispersal to Africa (*P* = 0.4792) from East Asia (freq. = 75.82%) at node 494 with a later dispersal to South America after the diversification of the genus *Eriochrysis* (Fig. S2).

Dispersal to Africa and West Asia from East Asia (freq. = 100%) was estimated by S-DIVA and DEC at node 485 (*P* = 1.0), including the unnamed clade consisting of *Microstegium*, *Sehima*, and *Kerriochloa* (Figs. 3A, S1). Dispersal to Africa from East Asia for this clade is placed at node 540 (as above) in the BBM analysis (Fig. S2).

The clade consisting of Rottboelliinae plus *Tripidium* had no estimated dispersal from East Asia to Africa during the Miocene using the S-DIVA analysis (Fig. 3A). The DEC analysis, however, suggests dispersal from East Asia (node 480; freq. = 86%) to Africa, West Asia, and Europe (*P* = 0.1711) (Fig. S1). The BBM analysis maintains the ancestral area of Africa + East Asia (freq. = 74.54%) from the original dispersal event characterized at node 540 (Fig. S2).

Following the S-DIVA and DEC analyses, the range of Ratzeburgiinae is estimated to be the result of dispersal from East Asia to Africa (node 482; *P* = 0.7090 [S-DIVA], 0.5399 [DEC]) followed by a vicariance event (node 481; *P* = 0.8512 [S-DIVA], 0.2181 [DEC]) (Figs. 3A, S1) where the lineage from which Ratzeburgiinae derives remains in Africa (S-DIVA freq. = 77.76%, BBM freq. = 94.03%) (Table 2). The DEC analysis found that Africa + East Asia had a higher frequency (52.2%) compared to just Africa (47.8%) for the ancestral area (Table 2). The BBM analysis estimated dispersal from East Asia to Africa much earlier (node 540; *P* = 0.4380) with an expanded range in Africa and East Asia until node 481 (*P* = 0.4204) where there was dispersal into a portion of Africa where the lineage was estimated to predominantly

**Table 2** Ancestral areas with frequencies, number of dispersal, vicariance, and extinction events, and putative RASP route, and marginal probability for main clades and subtribes of Andropogoneae as estimated by the statistical dispersal-vicariance (S-DIVA), dispersal-extinction-cladogenesis (DEC), and Bayesian Binary MCMC (BBM) models. Only ancestral areas with an estimated frequency of 1% or more are represented. Ancestral area designations are: A = Africa, B = Central America, C = East Asia, D = Europe, E = North America, F = Oceania, G = South America, and H = West Asia

| Taxonomic group | Node | Model | Ancestral area (percent frequency) | Dispersal events | Vicariance events | Extinction events | RASP route | *P* |
|---|---|---|---|---|---|---|---|---|
| Jansenelleae-Arundinelleae-Andropogoneae | 543 | S-DIVA | C 100.00 | 0 | 0 | 0 | C->C^C->C\|C | 1 |
| | | DEC | C 100.00 | 0 | 0 | 0 | C->C^C->C\|C | 1 |
| | | BBM | C 94.30, AC 2.55, BC 2.04 | 0 | 0 | 0 | C->C^C->C\|C | 0.6871 |
| Arundinelleae-Andropogoneae | 540 | S-DIVA | C 100.00 | 0 | 0 | 0 | C->C^C->C\|C | 1 |
| | | DEC | C 100.00 | 0 | 0 | 0 | C->C^C->C\|C | 1 |
| | | BBM | C 72.71, AC 21.75, CF 2.27, CH 1.38 | 1 | 0 | 0 | C->C^C->AC^C->C\|AC | 0.438 |
| Andropogoneae | 532 | S-DIVA | C 100.00 | 0 | 0 | 0 | C->C^C->C\|C | 1 |
| | | DEC | C 100.00 | 0 | 0 | 0 | C->C^C->C\|C | 1 |
| | | BBM | AC 74.88, C 12.76, ACH 9.57, CH 1.63 | 2 | 0 | 0 | AC->AC^A^C->AC\|AC | 0.3307 |
| Arthraxoninae | 529 | S-DIVA | C 100.00 | 0 | 0 | 0 | C->C^C->C\|C | 1 |
| | | DEC | C 100.00 | 0 | 0 | 0 | C->C^C->C\|C | 0.196 |
| | | BBM | AC 45.39, ACH 20.99, C 20.79, CH 9.61, ACF 1.36 | 2 | 0 | 0 | AC->AC^C->ACH^C->C\|ACH | 0.3662 |
| Tripsacinae | 524 | S-DIVA | B 100.00 | 0 | 0 | 0 | B->B^B->B\|B | 1 |
| | | DEC | B 67.33, BG 32.67 | 1 | 0 | 0 | B->B^B->BG^B->B\|BG | 0.5029 |
| | | BBM | B 71.99, BC 9.28, AB 8.51, BG 4.05, C 1.22, A 1.12, ABC 1.10 | 1 | 0 | 0 | B->B^B->BG^B->B\|BG | 0.6231 |
| Chionachninae | 501 | S-DIVA | C 100.00 | 0 | 0 | 0 | C->C^C->C\|C | 1 |
| | | DEC | C 100.00 | 0 | 0 | 0 | C->C^C->C\|C | 1 |
| | | BBM | C 95.79, AC 4.12 | 0 | 0 | 0 | C->C^C->C\|C | 0.9508 |
| Rhytachninae | 509 | S-DIVA | A 100.00 | 0 | 0 | 0 | A->A^A->A\|A | 1 |
| | | DEC | AC 68.50, A 31.50 | 1 | 0 | 0 | AC->AC^A->AC\|A | 0.4347 |
| | | BBM | AC 61.10, A 38.18 | 1 | 0 | 0 | AC->AC^A->AC\|A | 0.3559 |
| Chrysopogoninae | 497 | S-DIVA | C 100.00 | 0 | 0 | 0 | C->C^C->C\|C | 1 |
| | | DEC | C 100.00 | 0 | 0 | 0 | C->C^C->C\|C | 0.5337 |
| | | BBM | C 80.16, AC 19.11 | 0 | 0 | 0 | C->C^C->C\|C | 0.4319 |
| Rottboelliinae | 473 | S-DIVA | C 100.00 | 0 | 0 | 0 | C->C^C->C\|C | 1 |
| | | DEC | C 85.86, AC 14.14 | 2 | 0 | 0 | C->C^C->ACF^C->ACF\|C | 0.8586 |
| | | BBM | AC 58.46, C 27.89, ACF 8.98, CF 4.29 | 2 | 0 | 0 | AC->AC^C->ACF^C->ACF\|C | 0.5355 |
| Ratzeburgiinae | 467 | S-DIVA | A 77.76, ACG 11.14, AC 11.10 | 2 | 0 | 0 | A->A^A->ACG^A->A\|ACG | 0.3455 |
| | | DEC | AC 52.20, A 47.80 | 1 | 0 | 0 | AC->AC^A->A\|AC | 0.3004 |
| | | BBM | A 94.03, AC 5.35 | 0 | 0 | 0 | A->A^A->A\|A | 0.7341 |

Continued

**Table 2** Continued

| Taxonomic group | Node | Model | Ancestral area (percent frequency) | Dispersal events | Vicariance events | Extinction events | RASP route | *P* |
|---|---|---|---|---|---|---|---|---|
| Ischaeminae | 454 | S-DIVA | C 100.00 | 1 | 0 | 0 | C->C^C->AC^C->C\|AC | 1 |
| | | DEC | C 83.75, AC 16.25 | 1 | 0 | 0 | C->C^C->AC^C->C\|AC | 0.3845 |
| | | BBM | AC 45.01, C 40.69, ACF 6.29, CF 5.69, A 1.53 | 2 | 0 | 0 | C->C^C->ACF^C->CF\|AC | 0.095 |
| Germainiinae | 448 | S-DIVA | C 100.00 | 4 | 0 | 0 | C->C^C->ACDFH^C->ACDFH\|C | 1 |
| | | DEC | C 83.44, CF 16.56 | 4 | 0 | 0 | C->C^C->ACDFH^C->ACDFH\|C | 0.5863 |
| | | BBM | ACF 34.47, ACFH 28.90, CF 9.89, CFH 8.30, ACDF 4.19, ACDFH 3.51, AC 3.06, ACH 2.56, CDF 1.20, CDFH 1.01 | 4 | 0 | 0 | ACF->ACF^C^F->ACDFH^C^F->ACDFH\|CF | 0.1883 |
| Sorghinae | 428 | S-DIVA | C 100.00 | 2 | 0 | 0 | C->C^C->AC^C->AC\|C | 1 |
| | | DEC | AC 57.55, C 33.04, A 9.41 | 2 | 0 | 0 | AC->AC^C->AC\|C | 0.1395 |
| | | BBM | AC 91.12, A 3.64, ACH 2.73, C 1.62 | 2 | 0 | 0 | AC->AC^A^C->AC\|AC | 0.5599 |
| Saccharinae | 444 | S-DIVA | C 100.00 | 0 | 0 | 0 | C->C^C->C\|C | 1 |
| | | DEC | C 100.00 | 0 | 0 | 0 | C->C^C->C\|C | 0.761 |
| | | BBM | C 95.64, AC 3.94 | 0 | 0 | 0 | C->C^C->C\|C | 0.879 |
| Apludinae | 413 | S-DIVA | C 55.14, A 44.86 | 4 | 0 | 0 | C->C^A^C->ACFE^A^C->ACF\|ACE | 0.0298 |
| | | DEC | C 66.52, A 19.46, AC 14.02 | 2 | 0 | 0 | C->C^C->ACF^C->ACF\|C | 0.177 |
| | | BBM | AC 29.98, ACF 24.51, A 10.77, C 10.66, AF 8.81, CF 8.71, F 3.13 | 1 | 0 | 0 | AC->AC^C->AC\|C | 0.0117 |
| "core Andropogoneae" | 402 | S-DIVA | AC 100.00 | 0 | 1 | 0 | AC->C\|A | 1 |
| | | DEC | AC 100.00 | 0 | 1 | 0 | AC->C\|A | 1 |
| | | BBM | AC 41.42, A 33.44, ACF 9.19, AF 7.42, C 5.80, CF 1.29, F 1.04 | 0 | 1 | 0 | AC->C\|A | 0.1768 |
| Anthistiriinae | 401 | S-DIVA | C 100.00 | 0 | 0 | 0 | C->C^C->C\|C | 1 |
| | | DEC | C 100.00 | 0 | 0 | 0 | C->C^C->C\|C | 0.7633 |
| | | BBM | C 47.24, AC 26.17, CF 16.46, ACF 9.12 | 0 | 0 | 0 | C->C^C->C\|C | 0.164 |
| Andropogoninae | 373 | S-DIVA | A 100.00 | 0 | 0 | 0 | A->A^A->A\|A | 1 |
| | | DEC | A 100.00 | 0 | 0 | 0 | A->A^A->A\|A | 1 |
| | | BBM | A 90.94, AC 5.20, AF 3.35 | 0 | 0 | 0 | A->A^A->A\|A | 0.8887 |

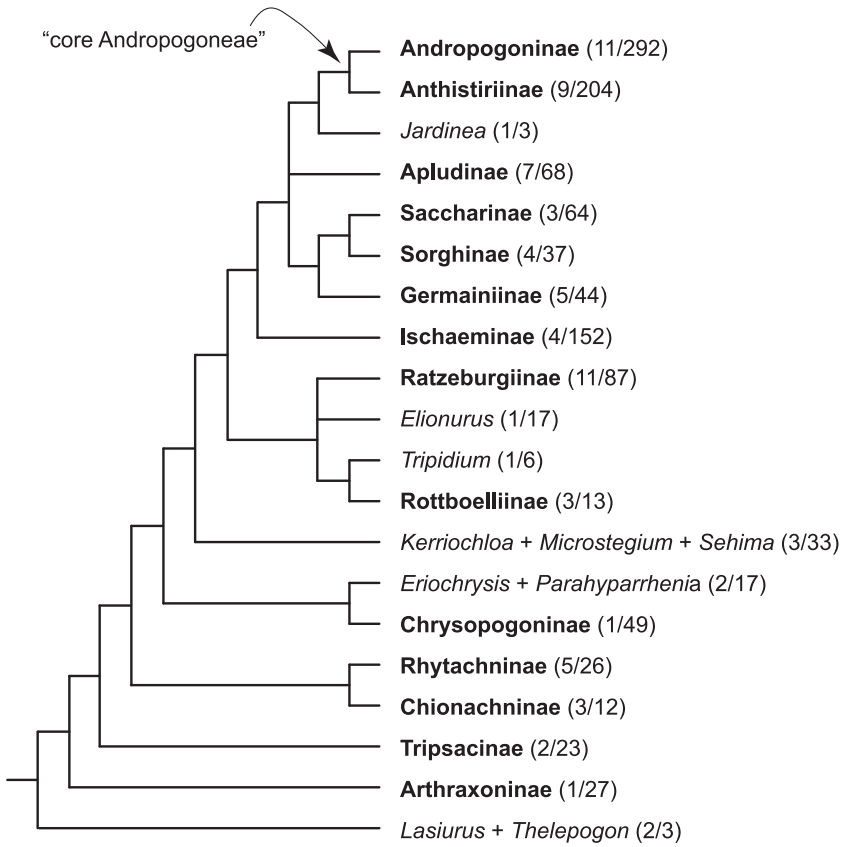


**Fig. 4.** Relationships among the subtribes and *incertae sedis* genera of Andropogoneae based on complete plastome sequences. The number of genera and species for each lineage is shown in parentheses. Subtribal names are highlighted in bold and the "core Andropogoneae" clade is indicated.

exist (node 469; Africa freq. = 74.57%) until dispersal back to East Asia followed by a vicariance event at node 466 ($P = 0.4596$) (Fig. S2).

The movement to Africa from East Asia was estimated at node 414 with S-DIVA ($P = 0.1073$) and DEC ($P = 0.3512$) before the diversification of the "core Andropogoneae" (node 402; S-DIVA freq. Africa + East Asia = 100%; DEC freq. Africa + East Asia = 100%) (Figs. 3B, S1; Table 2). This dispersal would also be the origin of members of the Apludinae in Africa. With the divergence of the Andropogoninae and Anthistiriinae, a vicariance event (node 402; S-DIVA and DEC $P = 1.0$) splits the ancestral area of Africa + East Asia (S-DIVA and DEC freq. = 100%) into Africa (Andropogoninae) and East Asia (Anthistiriinae). Again, the Africa + East Asia distribution leading to diversification of the "core Andropogoneae" is suggested to have originated right after the origin of the Andropogoneae (node 540) in the BBM analysis. A vicariance event at node 402 ($P = 0.1768$) then resulted in the aforementioned African and East Asian distributions of Andropogoninae and Anthistiriinae. Other movements into Africa likely occurred in Sorghinae (S-DIVA; $P = 1.0$) and Saccharinae (S-DIVA; $P = 1.0$) within the last 5 Ma (Fig. 3B).

Another major region for dispersal and subsequent diversification is the Western Hemisphere, here divided into North, Central, and South America. Up to six dispersals from the Eastern to the Western Hemisphere likely occurred during the Miocene: one in Tripsacinae, one in Ratzeburgiinae, one in Apludinae, and three in Andropogoninae with others occurring across the Andropogoneae during the last 5 Ma (Figs. 3, S1, S2).

The Tripsacinae represent one of the earliest movements into the Western Hemisphere by members of the Andropogoneae, though the estimated pathway of this movement varies among methods. The S-DIVA model estimated the ancestral area of the crown Tripsacinae (node 524) to be Central America (freq. = 100%; $P = 1.0$) (Table 2). No dispersal or vicariance event is estimated at node 524, but rather the presence of Tripsacinae in Central America contributed to a dispersal event from East Asia at node 530 ($P = 0.975$) followed by a vicariance event at node 525 ($P = 0.9263$) (Fig. 3A). The DEC model estimated the Tripsacinae crown ancestral area to be Central America (freq. = 67.33%) or Central America + South America (freq. = 32.67%) with a $P$ value of 0.5029 (Table 2). These estimates were the result of dispersal from East Asia to Central America followed by a vicariance event at node 525 ($P = 0.3892$), leaving what would become the Tripsacinae in Central Mexico. Postvicariance dispersal to South America is estimated at node 524 (Fig. S1). The BBM analysis also estimated the Tripsacinae crown ancestral area as Central America (freq. = 71.99%) with other possible ancestral areas also estimated for the node (e.g., Central America + East Asia: freq. = 9.28%; Central

America + Africa: freq = 8.51%; and Central America + South America: freq. = 4.05%) (Fig. S2; Table 2). In the BBM analysis, the presence of Tripsacinae in Central America is the result of dispersal to Africa early in the history of the tribe (node 540; $P = 0.4380$) followed by dispersal to Central America with a vicariance event leaving Tripsacinae to diversify in the Western Hemisphere (node 525; $P = 0.3683$) (Fig. S2).

The Ratzeburgiinae most recent common ancestor is node 467, which was estimated to have a dispersal event from Africa to East Asia and South America ($P = 0.3455$) from an ancestral area of Africa (freq. = 77.76%) by S-DIVA (Fig. 3A; Table 2). The DEC analysis suggested that node 467 had either an ancestral area of Africa + East Asia (freq. = 52.2%) or Africa (freq. = 47.8%), and the dispersal event to South America occurred at node 466 ($P = 0.3767$) (Fig. S1). BBM estimated dispersal later than both S-DIVA and DEC with the ancestral area at node 466 being Africa (freq. = 84.47%) with a dispersal to East Asia followed by a vicariance event ($P = 0.4596$) splitting the ranges. Movement into South America was not estimated until a dispersal event at node 456 from the ancestral area of Africa (freq. = 96.05%) followed by a vicariance event ($P = 0.9215$) during the last 2 Ma (Fig. S2).

The common ancestor of subtribe Apludinae is node 413, for which S-DIVA estimated dispersal from East Asia (freq. = 55.14%), though the ancestral area for the node may have been Africa (freq. = 44.86%), to a wide range of Africa, Oceania, and North America ($P = 0.0298$). This is followed by multiple vicariance events separating many of the lineages into single continent ranges (Fig. 3B). The DEC analysis suggests that dispersal from East Asia (freq. = 38.17%) to Africa, Oceania, North America, and West Asia occurred at node 410 along with a vicariance event separating lineages to Africa + North America and East Asia, West Asia, and Oceania ($P = 0.3197$) (Fig. S1). The BBM model suggests dispersal from Africa (freq. = 70.4%) to North America (node 408; $P = 0.6268$) with a vicariance event separating the lineages between the two continents (Fig. S2).

The Miocene Western Hemisphere dispersal events in the Andropogoninae are suggested to be from Africa to North America (node 340; $P = 0.3347$), Africa to Central and South America (node 301; $P = 0.333$), and Africa to South America (node 339; $P = 0.0669$) in the S-DIVA analysis (Fig. 3C). The dispersal at node 301 precedes diversification of the genus *Schizachyrium*, suggesting a South American origin of the genus. The DEC analysis suggests dispersal from Africa to North America (node 340; $P = 0.5237$), Africa to South America (node 301; $P = 0.3755$), and Africa to Central America, South America, East Asia, and West Asia (node 338; $P = 0.2282$) (Fig. S1). The BBM analysis identified dispersal events from Africa to Central and South America (node 298; $P = 0.1484$), from Africa to Central and South America (node 339; $P = 0.2684$), and Africa to North America (node 306; $P = 0.8698$) (Fig. S2).

### 3.5 New classification

Based on the present phylogenomic analyses, we propose a new classification of Andropogoneae composed of 14 subtribes (Appendix I). Two of them are new subtribes described in this paper (Chrysopogoninae and Rhytachninae; see Section 4.4) and most of the others have different circumscriptions compared to previous classifications. All subtribes have full support (100% MLBS, 1.0 BPP) in our plastome trees, except Ischaeminae (100% MLBS, 0.977 BPP) and Apludinae (98% MLBS, 0.638 BPP) (Fig. 2). Relationships among the subtribes (and *incertae sedis* genera of Andropogoneae) are summarized in Fig. 4, in which polytomies reflect the ambiguous placement of some taxa.

Our classification accepts 92 genera and ~1224 species in Andropogoneae. About half of the genera are small, with about a quarter including a single species, and another quarter having five species each or fewer. Only six genera (7%) comprise more than 50 species (see Appendix I). *Andropogon* is the type genus of the tribe and the largest one, with ~125 species, alone including about 10% of the species richness of Andropogoneae; however, it is clearly polyphyletic, so the apparently large size is almost certainly artifactual. In this classification, it was possible to place about 90% of the Andropogoneae species in one of the 14 subtribes, representing a major step toward clarification of the taxonomy of the tribe. The remaining species are kept *incertae sedis* here, pending additional molecular data. Genera not sampled in our plastome analyses and tentatively placed in subtribes based on previously published phylogenetic analyses or morphology are highlighted in Appendix I.

## 4 Discussion

### 4.1 Phylogeny of Andropogoneae

The phylogeny of Andropogoneae presented here includes the largest sample of the tribe so far, and confirms and extends data from previous studies. We have been able to resolve a number of previously poorly supported nodes in the early diversification of the tribe, presumably because our whole plastome dataset has more base pairs and more polymorphic sites than earlier works. In fact, the low resolution and poor support of the backbone of the Andropogoneae tree were the major challenge for inferring the phylogeny of the tribe in previous studies (e.g., Mathews et al., 2002; Teerawatananon et al., 2011; Estep et al., 2014; Welker et al., 2015). The increased resolution of the trees presented here, together with the large sample of genera, has allowed a deeper understanding of the evolution of the tribe and permitted a detailed subtribal classification. The 67 Andropogoneae genera included in our plastome analyses represent 73% of the 92 genera accepted in this new classification (Appendix I). For 76% of the sampled genera (51), we were able to include the type species, allowing confident decisions regarding the classification of the tribe. Nonetheless, a few parts of the tree remain poorly resolved and weakly supported, such as the relationship of *Elionurus* and the *Microstegium* clade to the clades that contain *Coix*, *Tripidium*, and *Mnesithea* (Fig. 2A). This part of the tree is resolved differently by ML analyses including and excluding gapped sites, but support is generally poor for any topology. Although the exclusion of gapped sites in the alignment has affected tree topologies in some other studies (Saarela et al., 2018; Duvall et al., 2020), we find that it does not influence the results here and in particular does not affect monophyly of the subtribes.

Most aspects of the plastome topology (Figs. 2, 3) are consistent with the topology provided by nuclear genes. We confirm here the sister position of the *Arundinella* clade to the tribe Andropogoneae, and *Arthraxon* as the only genus of an early-diverging lineage within Andropogoneae, in accordance with Estep et al. (2014). The clade formed by *Coix* and the type species of *Rottboellia* Naezén (*R. cochinchinensis*) is also strongly supported in nuclear phylogenies, as is the sister relationship of *Imperata* to the *Germainia-Pogonatherum* clade (Estep et al., 2014; Welker et al., 2015, 2016). We also confirm the presence of a "core Andropogoneae" clade formed by two internal clades treated here as the subtribes Anthistiriinae (which includes the informal "BCD" clade) and Andropogoninae (previously referred to as the "DASH" clade). These clades were recovered in recent nuclear phylogenies of Andropogoneae (Estep et al., 2014; Welker et al., 2015, 2016), although not always with full support as in our plastome trees. On the other hand, the position of *Chrysopogon* in a clade with *Eriochrysis* and *Parahyparrhenia* (Figs. 2A, 3A) is consistent with other plastome phylogenies of Andropogoneae (e.g., Arthan et al., 2017) but is clearly distinct from the topology provided by nuclear genes, in which *Chrysopogon* is sister to *Thelepogon* in a clade sister to all Andropogoneae except *Arthraxon* (Estep et al., 2014; Welker et al., 2015).

Our plastome phylogenies also indicate that several genera, such as *Andropogon*, *Schizachyrium*, *Eulalia*, and the genera of the "BCD" clade, need further taxonomic and phylogenetic attention since they do not form monophyletic groups in our trees (Figs. 2, 3). Both *Andropogon* and *Schizachyrium* appeared as polyphyletic in previous phylogenetic works (e.g., Arthan et al., 2017; McAllister et al., 2018), which was confirmed in this study. *Eulalia* was also clearly recovered as polyphyletic in recent nuclear (Estep et al., 2014; Welker et al., 2016) and plastome (Arthan et al., 2017) phylogenetic analyses, although only a couple of species were sampled in all these studies and in the present one. The intricate history of the "BCD" clade, which involves complex hybridization, polyploidy, and apomixis, has been known for half a century (Harlan & de Wet, 1963; de Wet & Harlan, 1970) and was investigated by Estep et al. (2014) using multiple low-copy nuclear genes, but can only be addressed by in-depth sampling in the native range of the species (South Asia, particularly Pakistan and India). Other genera with problems in their delimitations also demonstrated by our plastome analyses include *Cymbopogon*, *Elymandra*, *Heteropogon*, *Hyparrhenia*, *Loxodera*, *Miscanthus*, *Mnesithea*, *Saccharum*, and *Tripidium* (Figs. 2, 3). In all these cases, further studies with a broad sample of their species are required to better understand their circumscriptions. In the same way, the two accessions of some species are not sisters in our plastome trees. The discrepancies could be due to technical reasons (misidentification of vouchers, simple labeling mix-ups) or biological ones (hybridization, incomplete lineage sorting), but determining which would require a more detailed population-level study of the relevant species and genera.

Our dated phylogeny suggests that the divergence between Andropogoneae and Arundinelleae occurred in the Early Miocene, with the crown Andropogoneae taxa diverging in the Middle Miocene. The origin (crown node age) of the "core Andropogoneae" occurred in the Late Miocene (Fig. 3). The dates are similar to, although slightly younger than those suggested by the nuclear phylogeny of Estep et al. (2014). According to our dated phylogeny, most subtribes originated in the Late Miocene (crown node age), with the exception of Tripsacinae, Chionachninae, Rottboelliinae, Sorghinae, and Saccharinae originating in the Pliocene (Fig. 3; Table 1). This suggests that most Andropogoneae taxa diverged simultaneously with or following the expansion of the major $C_4$ grasslands of the world in the Late Miocene (Edwards et al., 2010), as previously described by Estep et al. (2014).

### 4.2 Biogeography

The Andropogoneae seem to have had two major periods of dispersal leading to their current global presence: the Late Miocene and the Pleistocene (Fig. 3). Likely originating in East Asia, as suggested by Hartley (1958), members of Andropogoneae have dispersed to both Africa and the Western Hemisphere multiple times via disparate routes. Not surprisingly, most dispersal events are documented in Eurasia, with fewer inferred to be trans-Pacific or trans-Atlantic. The center of diversity is thus in the Old World.

Frequent dispersal is not surprising in this group of grasses. The spikelets (flower- and seed-bearing structures) are light and often covered with hairs (see Fig. 1). In addition, the lemma (major bract) of most flowers bears an awn that extends beyond the rest of the bracts and may aid in reducing the terminal velocity of the spikelets and spikelet pairs, keeping them airborne for long periods of time (Clayton, 1969, 1972b; Clayton & Renvoize, 1986; Kellogg, 2015). While most species grow in open habitats and thus may be exposed to strong winds, some are aquatic and maybe water dispersed.

For the optimization of most ancestral nodes, we found broad agreement among the three models investigated. In general, the BBM model assigned more polymorphic states (i.e., multiple possible continents) to the ancestral node than the other two models, whereas the other two models assigned fewer states, but they tended to be a subset of those found by BBM. The BBM model also favored an ancient dispersal event from East Asia to Africa (Fig. S2) with a prolonged range consisting of both regions as opposed to the multiple dispersal events suggested by S-DIVA (Fig. 3) and DEC (Fig. S1) while more often maintaining smaller ranges.

Present-day Andropogoneae are widespread though their highest diversity is in the tropics and subtropics (Clayton & Renvoize, 1986). Andropogoneae likely originated in East Asia, near the time of the Miocene Climatic Optimum (MCO; ~17–14.7 Ma; Fig. 3A) and experienced novel increases in global atmospheric $CO_2$ concentrations during this period (Holbourn et al., 2015). Our estimations of ancestral areas suggest that the Andropogoneae remained in East Asia until after the Middle Miocene extinction peak (~11.3 Ma; Raup & Sepkoski Jr., 1984), which likely correlated with a rapid cooling event and decrease of global atmospheric $CO_2$ during the Middle Miocene Climate Transition (MMCT; Holbourn et al., 2005). For the S-DIVA and DEC analyses, the earliest movement from East Asia occurred sometime between 13 and 9 Ma (Figs. 3A, S1) where Tripsacinae and Rhytachninae

are expected to have dispersed to Central America and Africa, respectively. The BBM analysis, however, suggested that dispersal to Africa occurred prior to the diversification of Andropogoneae and much earlier (~17.5–14 Ma; Fig. S2), which would indicate a tropical expansion during the MCO and a later dispersal to Central America by the lineage leading to Tripsacinae (~13–5 Ma; Fig. S2). Although the various models suggest the same time frame for dispersal of Tripsacinae, they differ in the possible routes taken, whether directly from East Asia to Central America or from East Asia + Africa to Central America. The Tripsacinae lineage might have used the land bridge Beringia, which has been suggested as the source of many lineages in the Western Hemisphere flora (Graham, 2018), though the uncertainty in timing and ancestral range leaves this open to further study. Other post-MMCT Miocene dispersals occurred during and after the Miocene grassland expansion (~10–8 Ma; Edwards et al., 2010). Three estimated dispersals to Africa occurred during the grassland expansion: one before the divergence of *Elionurus* and Ratzeburgiinae (~9.5 Ma; Fig. 3A), one before the diversification of the "core Andropogoneae" (~9–8.6 Ma; Fig. 3B), and one after the origin of the Apludinae crown group (~8.4–7.4 Ma; Fig. 3B). The remaining dispersal events for the group occurred well after the putative grassland expansion, including into areas—South American Cerrado, North American Prairie, and Oceania (Australian Tussock grasslands)—where Andropogoneae are ecologically dominant. Understanding the rise of Andropogonean ecological dominance merits further investigation focusing on the Mid-Pliocene through the Pleistocene (last 4 Ma) and the numerous potential dispersal events that helped build the biodiversity of today's savannahs and other grasslands.

### 4.3 A new classification of Andropogoneae

The *Arundinella* clade, composed of the genera *Arundinella* and *Garnotia*, is accepted here as the tribe Arundinelleae, following Soreng et al. (2017) and Clayton & Renvoize (1986), and is confirmed as sister to the tribe Andropogoneae (Fig. 2A). In addition to these two genera, Soreng et al. (2017) included *Jansenella* in Arundinelleae, but this genus is now placed as the type of the recently described tribe Jansenelleae (Bianconi et al., 2020). Clayton & Renvoize (1986) also included nine other genera in Arundinelleae that are currently placed in Tristachyideae or Jansenelleae (Kellogg, 2015; Soreng et al., 2017; Bianconi et al., 2020).

The new classification of Andropogoneae presented here includes more subtribes (14; see Appendix I) than the treatments of Soreng et al. (2017), Kellogg (2015), and Clayton & Renvoize (1986), which included nine, seven, and 11 subtribes, respectively. Table S4 shows all accepted genera of Andropogoneae and their respective subtribes in our classification and in the treatments of Soreng et al. (2017), Kellogg (2015), and Clayton & Renvoize (1986). Relationships among the subtribes, based on our plastome analyses, are summarized in Fig. 4.

*Arthraxon* represents the single genus of the subtribe Arthraxoninae in our classification, as also accepted by Soreng et al. (2017). Clayton & Renvoize (1986) included *Arthraxon* in subtribe Andropogoninae, although they considered it "a homogeneous genus with (…) several unusual features which make it difficult to place in the system." Kellogg (2015) considered the genus *incertae sedis* in Andropogoneae. The acceptance here of this monogeneric subtribe is strongly justified since multiple phylogenetic analyses, based on both plastid and nuclear data, recover *Arthraxon* as an isolated lineage which is sister to the rest of Andropogoneae (e.g., GPWG II, 2012; Estep et al., 2014; Arthan et al., 2017).

*Arthraxon* has leaf blades with a cordate base (van Welzen, 1981), a character that Kellogg (2015) suggested might be synapomorphic, although this character is also shared with *Thelepogon* (Thompson, 2019). In addition, members of the genus have spikelets in which both florets generally lack paleas; the awn of the upper lemma is abaxial (rather than terminal), attached near the base of the lemma (van Welzen, 1981; Kellogg, 2015). *Arthraxon* is reported to have distinctive cells in its mesophyll (Ueno, 1995), similar to *Arundinella*, but to our knowledge, only a couple of species of the genus have been investigated. In addition, the basic chromosome number of $x = 9$ is unusual in a tribe that is otherwise mostly $x = 10$ (Clayton & Renvoize, 1986).

In this classification, subtribe Tripsacinae comprises only *Tripsacum* and *Zea*, in accordance with Clayton & Renvoize (1986) but differently from Kellogg (2015) and Soreng et al. (2017). The latter two treatments included some other genera in this subtribe, such as *Oxyrhachis*, *Rhytachne*, *Urelytrum*, and *Vossia*, which were placed in the subtribe Rottboelliinae by Clayton & Renvoize (1986). Our plastome analyses show that the latter four genera, together with *Loxodera*, in fact correspond to a clade distinct from *Tripsacum* and *Zea*, and also are separate from *Rottboellia s.s.* (Figs. 2A, 3A). Because of this structure, the new subtribe Rhytachninae is proposed herein to accommodate these five genera (see formal description in Section 4.4). *Loxodera* was previously placed in Rottboelliinae by Clayton & Renvoize (1986), Kellogg (2015), and Soreng et al. (2017).

Tripsacinae in a sense used here includes species with unisexual spikelets, in most cases borne in the same inflorescence with the pistillate spikelets below (proximal to) the staminate ones, although in the cultivated species *Zea mays* ssp. *mays*, the pistillate and staminate spikelets are in separate inflorescences (Doebley & Iltis, 1980; de Wet et al., 1981, 1982, 1983). While all spikelets originate in pairs, as in the remainder of Andropogoneae, in the pistillate portion of the inflorescence the pedicellate spikelet aborts while the sessile one matures to bear the seed (Sundberg & Orr, 1990; Orr & Sundberg, 1994; Orr et al., 2001). Pistillate spikelets are embedded in the rachis and the glumes, particularly the lower one, are indurate (Dorweiler & Doebley, 1997; Tian et al., 2002).

Rhytachninae all lack lemma awns, although many have awned (*Rhytachne*, *Urelytrum*) or caudate (*Vossia*) glumes (Clayton, 1973; Clayton & Renvoize, 1986; Watson & Dallwitz, 1992). Like *Zea* and *Tripsacum*, the glumes are indurate and the spikelets are more or less sunken the inflorescence axis. Many species are plants of wet sites, whether river banks (some *Urelytrum* and *Rhytachne*), swamps (*Oxyrhachis*), or shallow water (*Vossia*) (Clayton & Renvoize, 1982).

The subtribe Chionachninae includes here the genera *Chionachne*, *Polytoca*, and *Trilobachne* M. Schenck ex

Henrard; the latter is not sampled in our molecular analyses and is placed here based solely on morphology. The delimitation of the subtribe is similar to the treatments of Clayton & Renvoize (1986) and Soreng et al. (2017) except that they divided the genera more finely, also accepting *Sclerachne* R. Br. and/or *Cyathorhachis* Nees. Kellogg (2015) placed *Chionachne incertae sedis* in Andropogoneae based on its ambiguous position in phylogenetic trees (Teerawatananon et al., 2011; GPWG II, 2012; Estep et al., 2014), with the four genera mentioned above in its synonymy.

Like Tripsacinae, species of Chionachninae bear unisexual spikelets (Jannink & Veldkamp, 2002). The arrangement of the spikelets, however, is distinctive and probably synapomorphic. The pistillate spikelets are unpaired or paired with the pistillate spikelet sessile and the staminate one pedicellate. The distal part of the inflorescence bears paired staminate spikelets. The lower glumes of the pistillate spikelets are indurate, shining, and clasp the rachis, another derived character shared by members of the subtribe (Kellogg, 2015).

The genus *Chrysopogon* was included in the subtribe Sorghinae by Clayton & Renvoize (1986) but was placed *incertae sedis* in Andropogoneae by Kellogg (2015) and Soreng et al. (2017). Molecular data suggest that the evolutionary history of the *Chrysopogon* nucleus is different from that of the plastome. In nuclear trees, *Chrysopogon* is sister to *Thelepogon*, and this clade is sister to other Andropogoneae, excluding *Arthraxon* (Estep et al., 2014; Welker et al., 2015). In contrast, in plastome trees, including the one presented here (e.g., Arthan et al., 2017; Figs. 2A, 3A), *Chrysopogon* is firmly placed in a clade with *Eriochrysis* and *Parahyparrhenia*. Because the genus has its own history different from that of any other clades, and because the conflict between the trees indicates disparate placements, it seems plausible to include it in its own subtribe, Chrysopogoninae (see formal description in Section 4.4). The most distinctive character of *Chrysopogon* is that its spikelets are laterally, rather than dorsiventrally, compressed (Veldkamp, 1999). Kellogg (2015) suggested that this character might be a synapomorphy for the genus.

The subtribe Rottboelliinae has traditionally included several genera, such as *Rottboellia*, *Eremochloa*, *Glyphochloa*, *Hackelochloa*, *Hemarthria*, and *Mnesithea*, among others (Clayton & Renvoize, 1986; Kellogg, 2015; Soreng et al., 2017). On the other hand, the subtribe Coicinae included only the genus *Coix* in the treatments of Clayton & Renvoize (1986) and Soreng et al. (2017), while Kellogg (2015) placed *Coix incertae sedis* in Andropogoneae. However, our plastome trees clearly demonstrate that the type species of *Rottboellia* (*R. cochinchinensis*) is sister to *Coix* and not closely related to the other genera cited above (Figs. 2A, 3A). Therefore, the name Rottboelliinae is applied to the *Rottboellia-Coix* clade, since this name has nomenclatural priority over Coicinae. Although not sampled in our plastome trees, *Chasmopodium* Stapf is also included in this subtribe because the genus forms a strongly supported clade with *Rottboellia cochinchinensis* and *Coix* in nuclear phylogenies (e.g., Estep et al., 2014). Consequently, the circumscription of Rottboelliinae in this new classification is completely different from that adopted by previous treatments of the tribe, except by the presence of *Rottboellia cochinchinensis* and the genus *Chasmopodium* (Table S4). Several species formerly placed in *Rottboellia* (and accepted here under *Mnesithea*) do not belong to subtribe Rottboelliinae in this classification. In fact, it is possible that only *R. cochinchinensis* will end up in *Rottboellia*, but a phylogenetic analysis including all species of this group is needed to define it. On the other hand, there is an argument for recognizing Rottboelliinae and Coicinae as distinct subtribes; in this case, however, each of the subtribes would have only a few species and would provide no information on the phylogenetic relationship.

Since *Eremochloa*, *Glyphochloa*, *Hackelochloa*, *Hemarthria*, *Mnesithea*, and *Thyrsia* belong to a clade distinct from the one that comprises the type species of *Rottboellia* (Figs. 2A, 3A), the subtribe Ratzeburgiinae is accepted here to accommodate these genera. This subtribal name was originally proposed by Hooker (1896) to include only the genus *Ratzeburgia* Kunth, a classification that was not widely followed, and thus Ratzeburgiinae has been considered a synonym of Rottboelliinae (Clayton & Renvoize, 1986; Zuloaga et al., 2003). Here, the subtribe Ratzeburgiinae is resurrected and expanded considerably (see Appendix I). *Thyrsia* is often considered a synonym of *Phacelurus* Griseb. (e.g., Clayton & Renvoize, 1986; Soreng et al., 2017) but is accepted here as a separate genus since the type species of *Thyrsia* [*T. inflata* Stapf, a synonym of *Phacelurus huillensis* (Rendle) Clayton] is not closely related to the type of *Phacelurus* [*P. digitatus* (Sibth. & Sm.) Griseb.] in the nuclear phylogeny of Estep et al. (2014). A plastome sequence is not available for *Phacelurus s.s.*, so it is placed *incertae sedis* in this classification. In contrast, *Thyrsia* was included in the synonymy of *Rottboellia* by Kellogg (2015) but is clearly not related to the type species of *Rottboellia* either (Figs. 2A, 3A). *Heteropholis* C.E. Hubb., *Ophiuros* C.F. Gaertn., and *Thaumastochloa* C.E. Hubb. are also included in Ratzeburgiinae in this classification since they form a strongly supported clade with *Hemarthria* in GPWG II (2012). *Manisuris* L. is placed in this subtribe based on the phylogenetic analysis of Gosavi et al. (2016), while *Ratzeburgia* is placed here based solely on morphology. According to Clayton & Renvoize (1986), *Ratzeburgia* is "an elegant variant of the *Mnesithea* theme, in which the highly modified internode and pedicel form a narrow frame protecting the edges of the spikelets."

Generic limits in the Rottboelliinae and Ratzeburgiinae are famously complex, with morphological characters intergrading between species and genera; many species have names in several genera. Veldkamp et al. (1986) described the group as "a botanical black hole (…) the smaller and larger genera around the complex spiral down into making its mass even greater and its circumference even more difficult to envisage." His solution was to place species formerly assigned to *Coelorachis* Brongn., *Hackelochloa*, *Heteropholis*, *Ratzeburgia*, and *Rottboellia* in *Mnesithea*, although this suggestion has not been widely followed (see, e.g., Davidse et al., 1994; Barkworth et al., 2003; Arthan et al., 2016). All members of this group have unawned spikelets, with the sessile one generally sunken into the inflorescence axis, the glumes indurate, the pedicellate spikelet often reduced or lacking, and the pedicel sometimes entirely fused with the inflorescence axis (Clayton, 1973). Given the complex phylogeny of the awnless genera, it is unlikely that any of these characters are uniquely derived or diagnostic, since they are shared with *Rottboellia s.s.*, which

is unrelated, and many of the characters also appear in Tripsacinae and Rhytachninae.

The subtribe Ischaeminae comprises the genera *Andropterum*, *Dimeria*, *Eulaliopsis*, and *Ischaemum* in our classification. All these genera except *Eulaliopsis* were placed in this subtribe in the treatments of Kellogg (2015) and Soreng et al. (2017), whereas *Eulaliopsis* was treated as *incertae sedis* in both of them. Clayton & Renvoize (1986) accepted *Andropterum* and *Ischaemum* in Ischaeminae, *Dimeria* in the monogeneric subtribe Dimeriinae, and *Eulaliopsis* in Saccharinae (Table S4).

Ischaeminae lacks an obvious morphological synapomorphy (Kellogg, 2015), whether or not *Eulaliopsis* is included, although both spikelets are bisexual in *Eulaliopsis*, *Andropterum,* and some species of *Ischaemum* (Sur, 2001). *Dimeria* has solitary bisexual spikelets borne on short pedicels, suggesting a loss of the sessile spikelet, although Veldkamp (2016a) argues that the pedicellate spikelets may have been lost. Because of the loss of one spikelet of the pair, it is impossible to evaluate whether it was derived from an ancestor in which both spikelets were bisexual. *Eulaliopsis* also has unusual leaf anatomy, with the quaternary vascular bundles in rank below the tertiary ones (Renvoize, 1982); it is unclear whether other members of the subtribe have been examined for this character.

The subtribe Germainiinae was accepted by Kellogg (2015) and Soreng et al. (2017) with the same circumscription as in our classification except that we include *Imperata*, whereas those authors placed it in Saccharinae. Although the genus *Apocopis* Nees was not sampled in our plastome analyses, it is included here in this subtribe since previous phylogenetic works clearly place it in a clade with *Germainia* and *Pogonatherum* (Teerawatananon et al., 2011; Estep et al., 2014; Welker et al., 2016). These works also place *Imperata* sister to the *Apocopis-Germainia-Pogonatherum* clade, which is confirmed by our plastome analyses (Figs. 2B, 3B). The genus *Lophopogon* Hack., which has never been included in molecular phylogenies, is placed here in Germainiinae based only on morphology, in accordance with Kellogg (2015) and Soreng et al. (2017). This genus was included in Saccharinae by Clayton & Renvoize (1986), although they stated that *Lophopogon* "introduces a suite of characters—sterile basal spikelets, oblique pedicel tip, exserted upper glume and reduced floral parts—which are developed further in subtribe Germainiinae." Clayton & Renvoize (1986) also included *Trachypogon* in this subtribe, whereas it is placed in Apludinae in our classification (Table S4).

Kellogg (2015) listed the putative synapomorphies of Germainiinae (excluding *Imperata*) as having truncate glume apices, lodicules absent, two stamens, and papillae on the intercostal epidermal cells overarching the stomata. *Imperata* also lacks lodicules and has only one or two stamens per floret, providing some morphological support for its inclusion here. However, the glumes are obtuse to acuminate (not truncate), and the intercostal epidermal cells lack papillae (Watson & Dallwitz, 1992; Clayton et al., 2006 onwards).

Saccharinae and Sorghinae were considered distinct subtribes by Clayton & Renvoize (1986), while the latter was merged into the former in the classifications of Kellogg (2015) and Soreng et al. (2017). Our phylogenetic analyses indicate that the type genera of these subtribes (*Saccharum* and *Sorghum*, respectively) belong to two distinct clades, which are sister to each other in the plastome trees (Figs. 2B, 3B). However, these two clades were not recovered as sisters in nuclear phylogenies of Andropogoneae (e.g., Estep et al., 2014; Vorontsova et al., 2020). Because of this observation, plus the fact that Saccharinae *s.l.* (including Sorghinae) has no obvious morphological synapomorphies (Kellogg, 2015), here we accept Saccharinae and Sorghinae as distinct subtribes. It is important to emphasize that, although Clayton & Renvoize (1986) also accepted the two subtribes, their circumscriptions were substantially different than in our treatment, also including several genera that are placed here in the subtribes Anthistiriinae, Apludinae, Chrysopogoninae, Germainiinae, or Ischaeminae, or kept *incertae sedis* (Table S4). In our classification, the subtribe Saccharinae *s.s.* includes only three genera (*Saccharum*, *Miscanthus*, and *Pseudosorghum*) while Sorghinae includes four (*Sorghum*, *Cleistachne*, *Lasiorhachis*, and *Sarga*). The delimitations of the genera *Saccharum* and *Miscanthus* are controversial and largely unresolved (Hodkinson et al., 2002; Welker et al., 2015, 2019), so the number of genera accepted in Saccharinae may vary widely when new studies investigate their circumscriptions in depth.

In species of *Miscanthus* and *Saccharum* in Saccharinae *s.s.*, both spikelets of the pair are morphologically identical and generally have bisexual flowers. In contrast to most other Andropogoneae, the glumes are flimsy, either membranous or papery. The base of the spikelet (callus) bears hairs that are often as long as or longer than the spikelet (Mukherjee, 1958; Watson & Dallwitz, 1992; Sun et al., 2010; Welker et al., 2017). *Pseudosorghum* does not fit this description of Saccharinae and indeed looks more like sorghum, as its name suggests. However, it is well-supported in its position as sister to the rest of the subtribe in the present analysis as well as that of Vorontsova et al. (2020). Sorghinae do not have any obvious morphological synapomorphy.

The genera *Apluda*, *Eulalia s.s.* (here represented solely by the type, *E. aurea*), *Homozeugos*, *Polytrias*, *Sorghastrum*, and *Trachypogon* here form a clade distinct from Saccharinae and Sorghinae. This clade is recovered as sister to the Germainiinae-Saccharinae-Sorghinae clade in our ML tree (Fig. 2B) but as sister to the "core Andropogoneae" clade plus *Jardinea* in our Bayesian tree (Fig. 3B), in none of them with high support. The subtribe Apludinae, originally proposed by Hooker (1896) as a monogeneric subtribe including only *Apluda*, is accepted in this classification in a broader sense to accommodate the six genera cited above plus *Asthenochloa* Buse, placed here due to its morphological similarity to *Sorghastrum* (Appendix I). Clayton & Renvoize (1986) described *Asthenochloa* as "a segregate from *Sorghastrum*, distinguished by its keeled upper glume and reduced floral parts." All seven genera accepted here in Apludinae were included in Saccharinae by Soreng et al. (2017), except *Apluda*, which was considered *incertae sedis*. Kellogg (2015) placed *Homozeugos* and *Trachypogon* in the subtribe Andropogoninae, and the remaining genera in Saccharinae or *incertae sedis* (Table S4). The genus *Agenium*, not sampled in our plastome analyses, was suggested in the past to be closely related to *Homozeugos* and *Trachypogon* by morphological cladistic analysis (Kellogg & Watson, 1993) and a very limited molecular study (Guala, 2000). However, as *Agenium* has not been included in any recent phylogeny of

Andropogoneae and its placement in Apludinae cannot be strongly justified by morphology, we prefer to keep it *incertae sedis* pending further investigation. *Agenium* was included in the subtribes Saccharinae, Andropogoninae, and Anthistiriinae by Soreng et al. (2017), Kellogg (2015), and Clayton & Renvoize (1986), respectively, which highlights the uncertainty regarding its placement.

The genera of Apludinae apparently have little in common morphologically (Watson & Dallwitz, 1992; Clayton et al., 2006 onwards). *Polytrias* and *Apluda* have spikelets in threes, whereas the other species have more conventional pairs. All spikelets are bisexual in *Eulalia*, *Homozeugos*, and *Polytrias* (generally). The pedicellate spikelet is also bisexual in *Trachypogon*, but the sessile one is reduced (contra the more usual arrangement), and in *Sorghastrum* and *Asthenochloa*, the pedicellate spikelet is absent or reduced (Clayton & Renvoize, 1986; Watson & Dallwitz, 1992).

Clayton & Renvoize (1986) considered Andropogoninae and Anthistiriinae as two distinct subtribes, while the latter was merged into the former in the treatments of Kellogg (2015) and Soreng et al. (2017). The large clade including both subtribes was referred to by some authors as "core Andropogoneae" (e.g., Mathews et al., 2002; Estep et al., 2014; Welker et al., 2016; Arthan et al., 2017), and is monophyletic in all molecular phylogenetic analyses to date. With current data, this broadly circumscribed Andropogoninae now appears to be a large and rather unwieldy group, encompassing almost half of the tribe. As this group is formed by two strongly supported clades, each with a large number of species and including the type genus of Andropogoninae (*Andropogon*) and Anthistiriinae (*Anthistiria* Naezén, a synonym of *Themeda*) (Figs. 2B, 2C, 3B, 3C), respectively, we accept Anthistiriinae as distinct from Andropogoninae for convenience. Although Clayton & Renvoize (1986) also accepted Anthistiriinae, their circumscription of the subtribe is quite different from that presented here, except by the presence of *Themeda*, *Heteropogon*, and *Iseilema*. Most other genera accepted by Clayton & Renvoize (1986) in Anthistiriinae are placed here in Andropogoninae (Table S4). Anthistiriinae comprises nine genera in this classification (see Appendix I), including *Bothriochloa*, *Capillipedium*, and *Dichanthium*, which form the "BCD" clade of Estep et al. (2014). Although not sampled in our plastome analyses, *Eremopogon* Stapf is also placed in this subtribe since it is clearly nested in the Anthistiriinae clade in the nuclear trees of Estep et al. (2014).

In our classification, Andropogoninae includes 10 genera, all of them placed in this subtribe in the treatments of Kellogg (2015) and Soreng et al. (2017). The lineage that forms this subtribe was informally referred to as the "DASH" clade by Arthan et al. (2017) and McAllister et al. (2018) in reference to its main genera *Diheteropogon*, *Andropogon*, *Schizachyrium*, and *Hyparrhenia*. *Andropogon* is the largest genus of the tribe, including more than one hundred species, but is clearly polyphyletic with species scattered throughout the Andropogoneae (Figs. 2, 3). We expect many changes in the generic circumscription in Andropogoninae when future phylogenetic studies cover all species of this clade, possibly increasing the number of genera accepted. The genus *Bhidea* Stapf ex Bor was not sampled in our analyses and is placed here based only on morphology. According to Clayton & Renvoize (1986), "the genus is a peripheral segregate from *Andropogon* sect. *Andropogon*, barely deserving separate recognition."

Neither Anthistiriinae nor Andropogoninae has obvious shared derived morphological characters. In several members of Anthistiriinae, the basal (proximal) portion of the inflorescence bears pairs of staminate or sterile spikelets, also known as homogamous pairs. These are most obvious in species of *Heteropogon*, where there may be many such pairs, but they also occur in *Themeda* and *Iseilema*, where they form an involucre (Watson & Dallwitz, 1992; Clayton et al., 2006 onward). In most species of *Cymbopogon*, the lower of the two inflorescence branches also bears a homogamous pair (Soenarko, 1977). However, members of the "BCD" clade lack such pairs entirely (Clayton & Renvoize, 1986; Watson & Dallwitz, 1992), so the character is not diagnostic for Anthistiriinae. Kellogg (2015) also suggested that the presence of papillae on intercostal epidermal cells could be shared and synapomorphic among some genera now placed in Anthistiriinae, but this needs to be examined on a wider sample of species.

### 4.4 New subtribal names

Based on our results, and meeting the criteria described above, two new subtribes are proposed herein.

**Chrysopogoninae** Welker & E.A. Kellogg, **subtribe nov.**

**Type:** *Chrysopogon* Trin., Fund. Agrost. 187. 1820.

**Description:** Plants perennial, rarely annual, caespitose, rhizomatous, or stoloniferous. Ligules membranous, membranous-ciliate, or a fringe of hairs. Leaf-blades linear, lanceolate, or filiform. Inflorescence terminal, paniculate, with primary branches, generally whorled along the central axis, each bearing a raceme. Racemes with paired spikelets at each node of the rachis, 1 sessile and 1 pedicellate (except at the apex of the racemes, with a triad of 1 sessile and 2 pedicellate spikelets), sometimes reduced to the terminal triad; spikelets not sunken in the rachis. Rachis fragile and disarticulating at the nodes. Sessile spikelets laterally compressed, with 2 florets; callus generally pungent, bearded; lower glume without keels, generally not sculptured; lower floret neuter; upper floret bisexual; upper lemma awned, the awn apical or from a sinus, rarely muticous. Pedicellate spikelets well-developed or rudimentary, staminate or neuter; pedicel free of the rachis.

**Included genus:** *Chrysopogon*

**Distribution:** Tropical and subtropical regions of the world, especially in Asia and Oceania.

**Rhytachninae** Welker & E.A. Kellogg, **subtribe nov.**

**Type:** *Rhytachne* Desv. ex Ham., Prodr. Pl. Ind. Occid. xiv, 11. 1825.

**Description:** Plants perennial, less commonly annual, caespitose, or rhizomatous. Ligules membranous or membranous-ciliate. Leaf-blades linear or filiform. Inflorescence terminal, composed of a single raceme, less commonly with racemes paired, digitate, or borne along a central axis. Racemes with paired spikelets at each node of the rachis, 1 sessile and 1 pedicellate (except at the apex of the racemes, with a triad of 1 sessile and 2 pedicellate spikelets), rarely with solitary sessile spikelets (*Oxyrhachis*), never reduced to the terminal triad;

spikelets generally sunken in the rachis. Rachis fragile and disarticulating at the nodes. Sessile spikelets dorsiventrally compressed, with 2 florets; callus truncate or obtuse, glabrous, pubescent, or bearded; lower glume without keels, less commonly 2-keeled, sometimes sculptured; lower floret neuter or staminate; upper floret bisexual; upper lemma muticous. Pedicellate spikelets well-developed, rudimentary, represented by a barren pedicel, or absent, neuter, staminate, or bisexual; pedicel free of the rachis, rarely fused to and indistinguishable from the rachis internode (*Oxyrhachis*).

**Included genera:** *Loxodera*, *Oxyrhachis*, *Rhytachne*, *Urelytrum*, and *Vossia*.

**Distribution:** Tropical regions of the world, especially in Africa.

**Observation:** Although Stapf (1917) proposed the name "Vossiastrae" for a group of genera that includes *Vossia*, the name is unranked (Zuloaga et al., 2003) and therefore not applicable for this subtribe.

## Acknowledgements

This study was supported by the National Science Foundation (NSF, USA) Grants DEB-11456884 and DEB-1457748 to Elizabeth A. Kellogg. The authors would like to thank Jefferson Prado and Kanchi N. Gandhi for discussions on nomenclature, Riccardo Baldini for providing herbarium samples for DNA extraction, Simon Malcomber for the collection of multiple specimens critical for the analysis, and Jordan Brock, Andrew Doust, Carolline Z. Fieker, John Hodge, and Hilda M. Longhi-Wagner for providing photos of Andropogoneae. Cassiano A. D. Welker would like to thank Conselho Nacional de Desenvolvimento Científico e Tecnológico (CNPq, Brazil) for grants and fellowships (426334/2018-3 and 150896/2019-0) and the Smithsonian Institution, Missouri Botanical Garden, and Harvard University for travel grants to visit and curate their herbarium collections (Cuatrecasas Award, Shirley A. Graham Fellowship in Systematic Botany and Biogeography, and Harvard University Herbaria Travel Grant, respectively).

## References

Ali SS, Yu Y, Pfosser M, Wetschnig W. 2012. Inferences of biogeographical histories within subfamily Hyacinthoideae using S-DIVA and Bayesian binary MCMC analysis implemented in RASP (Reconstruct Ancestral State in Phylogenies). *Annals of Botany* 109: 95–107.

Arthan W, McKain MR, Traiperm P, Welker CAD, Teisher JK, Kellogg EA. 2017. Phylogenomics of Andropogoneae (Panicoideae: Poaceae) of mainland Southeast Asia. *Systematic Botany* 42: 418–431.

Arthan W, Traiperm P, Gale SW, Norsaengsri M, Kethirun L. 2016. Re-evaluation of the taxonomic status of *Hackelochloa* (Poaceae) based on anatomical and phenetic analyses. *Botanical Journal of the Linnean Society* 181: 224–245.

Bankevich A, Nurk S, Antipov D, Gurevich AA, Dvorkin M, Kulikov AS, Lesin VM, Nikolenko SI, Pham S, Prjibelski AD, Pyshkin AV, Sirotkin AV, Vyahhi N, Tesler G, Alekseyev MA, Pevzner PA. 2012. SPAdes: A new genome assembly algorithm and its applications to single-cell sequencing. *Journal of Computational Biology* 19: 455–477.

Barkworth ME, Capels KM, Long S, Piep MB eds. 2003. *Flora of North America north of Mexico. Vol. 25. Magnoliophyta: Commelinidae (in part): Poaceae, Part 1*. New York: Oxford University Press.

Besnard G, Christin PA, Malé PJG, Coissac E, Ralimanana H, Vorontsova MS. 2013. Phylogenomics and taxonomy of Lecomtelleae (Poaceae), an isolated panicoid lineage from Madagascar. *Annals of Botany* 112: 1057–1066.

Bianconi ME, Hackel J, Vorontsova MS, Alberti A, Arthan W, Burke SV, Duvall MR, Kellogg EA, Lavergne S, McKain MR, Meunier A, Osborne CP, Traiperm P, Christin PA, Besnard G. 2020. Continued adaptation of $C_4$ photosynthesis after an initial burst of changes in the Andropogoneae grasses. *Systematic Biology* 69: 445–461.

Bolger AM, Lohse M, Usadel B. 2014. Trimmomatic: A flexible trimmer for Illumina sequence data. *Bioinformatics* 30: 2114–2120.

Bouchenak-Khelladi Y, Verboom GA, Savolainen V, Hodkinson TR. 2010. Biogeography of the grasses (Poaceae): A phylogenetic approach to reveal evolutionary history in geographical space and geological time. *Botanical Journal of the Linnean Society* 162: 543–557.

Bouckaert R, Heled J, Kühnert D, Vaughan T, Wu C-H, Xie D, Suchard MA, Rambaut A, Drummond AJ. 2014. BEAST 2: A software platform for Bayesian evolutionary analysis. *PLoS Computational Biology* 10: e1003537.

Burke SV, Wysocki WP, Zuloaga FO, Craine JM, Pires JC, Edger PP, Mayfield-Jones D, Clark LG, Kelchner SA, Duvall MR. 2016. Evolutionary relationships in Panicoid grasses based on plastome phylogenomics (Panicoideae; Poaceae). *BMC Plant Biology* 16: 140.

Christin PA, Spriggs E, Osborne CP, Strömberg CAE, Salamin N, Edwards EJ. 2014. Molecular dating, evolutionary rates, and the age of the grasses. *Systematic Biology* 63: 153–165.

Clayton WD. 1969. *A revision of the genus* Hyparrhenia. Kew Bulletin Additional Series 11. Kew: Her Majesty's Stationery Office.

Clayton WD. 1972a. Gramineae. In: Hepper FN ed. *Flora of west tropical Africa*. London: Crown Agents for Oversea Governments and Administrations. 3: 349–512.

Clayton WD. 1972b. The awned genera of Andropogoneae. Studies in the Gramineae: XXXI. *Kew Bulletin* 27: 457–474.

Clayton WD. 1973. The awnless genera of Andropogoneae. Studies in the Gramineae: XXXIII. *Kew Bulletin* 28: 49–57.

Clayton WD, Renvoize SA. 1982. Gramineae (Part 3). In: Polhill RM ed. *Flora of tropical East Africa*. Rotterdam: A.A. Balkema. 451–898.

Clayton WD, Renvoize SA. 1986. *Genera graminum: Grasses of the world*. London: Her Majesty's Stationery Office.

Clayton WD, Vorontsova MS, Harman KT, Williamson H. 2006. GrassBase—The Online World Grass Flora: The Board of Trustees, Royal Botanic Gardens [online]. Available from http://www.kew.org/data/grasses-db.html [accessed 10 January 2020].

Darriba D, Posada D, Kozlov AM, Stamatakis A, Morel B, Flouri T. 2020. ModelTest-NG: A new and scalable tool for the selection of DNA and protein evolutionary models. *Molecular Biology and Evolution* 37: 291–294.

Davidse G, Sousa M, Chater AO. 1994. *Flora mesoamericana: Alismataceae a Cyperaceae*. Mexico City: Universidad Nacional Autónoma de México. 6.

Day R, Abrahams P, Bateman M, Beale T, Clottey V, Cock M, Colmenarez Y, Corniani N, Early R, Godwin J, Gomez J, Moreno PG, Murphy ST, Oppong-Mensah B, Phiri N, Pratt C, Silvestri S, Witt A. 2017. Fall armyworm: Impacts and implications for Africa. *Outlooks on Pest Management* 28: 196–201.

de Wet JMJ, Brink DE, Cohen CE. 1983. Systematics of *Tripsacum* section *Fasciculata* (Gramineae). *American Journal of Botany* 70: 1139–1146.

de Wet JMJ, Harlan JR. 1970. Apomixis, polyploidy, and speciation in *Dichanthium*. *Evolution* 24: 270–277.

de Wet JMJ, Harlan JR, Brink DE. 1982. Systematics of *Tripsacum dactyloides* (Gramineae). *American Journal of Botany* 69: 1251–1257.

de Wet JMJ, Timothy DH, Hilu KW, Fletcher GB. 1981. Systematics of South American *Tripsacum* (Gramineae). *American Journal of Botany* 68: 269–276.

Doebley JF, Iltis HH. 1980. Taxonomy of *Zea* (Gramineae). I. A subgeneric classification with key to taxa. *American Journal of Botany* 67: 982–993.

Dorweiler JE, Doebley J. 1997. Developmental analysis of *Teosinte glume architecture1*: A key locus in the evolution of maize (Poaceae). *American Journal of Botany* 84: 1313–1322.

Doyle JJ, Doyle JL. 1987. A rapid DNA isolation procedure for small quantities of fresh leaf tissue. *Phytochemical Bulletin* 19: 11–15.

Duvall MR, Burke SV, Clark DC. 2020. Plastome phylogenomics of Poaceae: Alternate topologies depend on alignment gaps. *Botanical Journal of the Linnean Society* 192: 9–20.

Edwards EJ, Osborne CP, Strömberg CAE, Smith SA, $C_4$ Grasses Consortium. 2010. The origins of $C_4$ grasslands: Integrating evolutionary and ecosystem science. *Science* 328: 587–591.

Estep MC, McKain MR, Vela Diaz D, Zhong J, Hodge JG, Hodkinson TR, Layton DJ, Malcomber ST, Pasquet R, Kellogg EA. 2014. Allopolyploidy, diversification, and the Miocene grassland expansion. *Proceedings of the National Academy of Sciences USA* 111: 15149–15154.

Gosavi KVC, Yadav SR, Karanth KP, Surveswaran S. 2016. Molecular phylogeny of *Glyphochloa* (Poaceae, Panicoideae), an endemic grass genus from the Western Ghats, India. *Journal of Systematics and Evolution* 54: 162–174.

Gould FW. 1972. A systematic treatment of *Garnotia* (Gramineae). *Kew Bulletin* 27: 515–562.

GPWG (Grass Phylogeny Working Group) II. 2012. New grass phylogeny resolves deep evolutionary relationships and discovers $C_4$ origins. *New Phytologist* 193: 304–312.

Graham A. 2018. The role of land bridges, ancient environments, and migrations in the assembly of the North American flora. *Journal of Systematics and Evolution* 56: 405–429.

Guala GF. 2000. The relation of space and geography to cladogenic events in *Agenium* and *Homozeugos* (Poaceae: Andropogoneae) in South America and Africa. In: Jacobs SWL, Everett J eds. *Grasses: Systematics and evolution*. Melbourne: CSIRO. 159–166.

Harlan JR, de Wet JMJ. 1963. The compilospecies concept. *Evolution* 17: 497–501.

Hartley W. 1958. Studies on the origin, evolution and distribution of the Gramineae. I. The tribe Andropogoneae. *Australian Journal of Botany* 6: 116–128.

Hodkinson TR, Chase MW, Lledó DM, Salamin N, Renvoize SA. 2002. Phylogenetics of *Miscanthus*, *Saccharum* and related genera (Saccharinae, Andropogoneae, Poaceae) based on DNA sequences from ITS nuclear ribosomal DNA and plastid *trnL* intron and *trnL-F* intergenic spacers. *Journal of Plant Research* 115: 381–392.

Holbourn A, Kuhnt W, Kochhann KGD, Andersen N, Sebastian, Meier KJ. 2015. Global perturbation of the carbon cycle at the onset of the Miocene Climatic Optimum. *Geology* 43: 123–126.

Holbourn A, Kuhnt W, Schulz M, Erlenkeuser H. 2005. Impacts of orbital forcing and atmospheric carbon dioxide on Miocene ice-sheet expansion. *Nature* 438: 483–487.

Hooker JD. 1896. *Flora of British India*. London: L. Reeve & Co. VII.

Jannink TA, Veldkamp JF. 2002. Revision of Chionachninae (Gramineae: Andropogoneae). *Blumea* 47: 545–580.

Judziewicz EJ. 1990. Poaceae (Gramineae). In: Görts-van Rijn ARA ed. *Flora of the Guianas, Series A: Phanerogams, Fascicle 8*. Koenigstein: Koeltz Scientific Books. 1–727.

Katoh K, Standley DM. 2013. MAFFT multiple sequence alignment software version 7: Improvements in performance and usability. *Molecular Biology and Evolution* 30: 772–780.

Kellogg EA. 2015. Poaceae. In: Kubitzki K ed. *The families and genera of vascular plants*, XIII. Cham: Springer International. 1–416.

Kellogg EA, Watson L. 1993. Phylogenetic studies of a large data set. I. Bambusoideae, Andropogonodae, and Pooideae (Gramineae). *The Botanical Review* 59: 273–343.

Lanfear R, Calcott B, Kainer D, Mayer C, Stamatakis A. 2014. Selecting optimal partitioning schemes for phylogenomic datasets. *BMC Evolutionary Biology* 14: 82.

Lanfear R, Frandsen PB, Wright AM, Senfeld T, Calcott B. 2017. PartitionFinder 2: New methods for selecting partitioned models of evolution for molecular and morphological phylogenetic analyses. *Molecular Biology and Evolution* 34: 772–773.

Langmead B, Salzberg SL. 2012. Fast gapped-read alignment with Bowtie 2. *Nature Methods* 9: 357–359.

Le Ru BP, Capdevielle-Dulac C, Conlong D, Pallangyo B, van den Berg J, Ong'amo G, Kergoat GJ. 2015. A revision of the genus *Conicofrontia* Hampson (Lepidoptera, Noctuidae, Apameini, Sesamiina), with description of a new species: New insights from morphological, ecological and molecular data. *Zootaxa* 3925: 56–74.

Le Ru BP, Capdevielle-Dulac C, Musyoka BK, Pallangyo B, Njaku M, Mubenga O, Chipabika G, Ndemah R, Bani G, Molo R, Ong'amo G, Kergoat GJ. 2017. Phylogenetic analysis and systematics of the *Acrapex unicolora* Hampson species complex (Lepidoptera, Noctuidae, Noctuinae, Apameini), with the description of five new species from the Afrotropics. *European Journal of Taxonomy* 270: 1–36.

Linder HP, Lehmann CER, Archibald S, Osborne CP, Richardson DM. 2018. Global grass (Poaceae) success underpinned by traits facilitating colonization, persistence and habitat transformation. *Biological Reviews* 93: 1125–1144.

Lloyd Evans D, Joshi SV, Wang J. 2019. Whole chloroplast genome and gene locus phylogenies reveal the taxonomic placement and relationship of *Tripidium* (Panicoideae: Andropogoneae) to sugarcane. *BMC Evolutionary Biology* 19: 33.

Mathews S, Spangler RE, Mason-Gamer RJ, Kellogg EA. 2002. Phylogeny of Andropogoneae inferred from phytochrome B, GBSSI and *ndhF*. *International Journal of Plant Science* 163: 441–450.

McAllister CA, McKain MR, Li M, Bookout B, Kellogg EA. 2018. Specimen-based analysis of morphology and the environment in ecologically dominant grasses: The power of the herbarium. *Philosophical Transactions of the Royal Society B* 374: 20170403.

McKain MR, Hartsock RH, Wohl MM, Kellogg EA. 2017a. Verdant: Automated annotation, alignment and phylogenetic analysis of whole chloroplast genomes. *Bioinformatics* 33: 130–132.

McKain MR, McNeal JR, Kellar PR, Eguiarte LE, Pires JC, Leebens-Mack J. 2016. Timing of rapid diversification and convergent origins of active pollination within Agavoideae (Asparagaceae). *American Journal of Botany* 103: 1717–1729.

McKain MR, Wilson M, Kellogg EA. 2017b. Fast-Plast (all versions). Zenodo. Available from https://doi.org/10.5281/zenodo.597709 [accessed 23 January 2020].

Miller MA, Pfeiffer W, Schwartz T. 2010. Creating the CIPRES Science Gateway for inference of large phylogenetic trees. In:

Proceedings of the Gateway Computing Environments Workshop, New Orleans, LA. 1–8.

Morrone O, Aagesen L, Scataglini MA, Salariato DL, Denham SS, Chemisquy MA, Sede SM, Giussani LM, Kellogg EA, Zuloaga FO. 2012. Phylogeny of the Paniceae (Poaceae: Panicoideae): Integrating plastid DNA sequences and morphology into a new classification. *Cladistics* 28: 333–356.

Mukherjee SK. 1958. Revision of the genus *Erianthus* Michx. (Gramineae). *Lloydia* 21: 157–188.

Orr AR, Kaparthi R, Dewald CL, Sundberg MD. 2001. Analysis of inflorescence organogenesis in eastern gamagrass, *Tripsacum dactyloides* (Poaceae): The wild type and the gynomonoecious *gsf1* mutant. *American Journal of Botany* 88: 363–381.

Orr AR, Sundberg MD. 1994. Inflorescence development in a perennial teosinte: *Zea perennis* (Poaceae). *American Journal of Botany* 81: 598–608.

Peichoto MC. 2013. Nota sobre el género *Imperata* (Poaceae, Panicoideae, Sacchareae) en Argentina. *Darwiniana* 1: 20–24.

Prasad V, Strömberg CAE, Alimohammadian H, Sahni A. 2005. Dinosaur coprolites and the early evolution of grasses and grazers. *Science* 310: 1177–1180.

Prasad V, Strömberg CAE, Leaché AD, Samant B, Patnaik R, Tang L, Mohabey DM, Ge S, Sahni A. 2011. Late Cretaceous origin of the rice tribe provides evidence for early diversification in Poaceae. *Nature Communications* 2: 480.

Rambaut A, Drummond AJ, Xie D, Baele G, Suchard MA. 2018. Tracer v.1.7.1. http://beast.community/tracer [accessed 23 February 2020].

Raup DM, Sepkoski JJ, Jr. 1984. Periodicity of extinctions in the geologic past. *Proceedings of the National Academy of Sciences USA* 81: 801–805.

Ree RH, Smith SA. 2008. Maximum likelihood inference of geographic range evolution by dispersal, local extinction, and cladogenesis. *Systematic Biology* 57: 4–14.

Renvoize SA. 1982. A survey of leaf-blade anatomy in grasses. I. Andropogoneae. *Kew Bulletin* 37: 315–321.

Reveal JL. 2004. *Earlier validation of certain tribal names in Poaceae*. Latest News on Vascular Plant Family Nomenclature. University of Maryland. [online]. Available from http://www.plantsystematics.org/reveal/pbio/fam/NEWS.html [accessed 10 January 2020].

Ronquist F, Huelsenbeck JP. 2003. MrBayes 3: Bayesian phylogenetic inference under mixed models. *Bioinformatics* 19: 1572–1574.

Saarela JM, Burke SV, Wysocki WP, Barrett MD, Clark LG, Craine JM, Peterson PM, Soreng RJ, Vorontsova MS, Duvall MR. 2018. A 250 plastome phylogeny of the grass family (Poaceae): Topological support under different data partitions. *PeerJ* 6: e4299.

Sánchez-Ken JG, Clark LG. 2010. Phylogeny and a new tribal classification of the Panicoideae *s.l.* (Poaceae) based on plastid and nuclear sequence data and structural data. *American Journal of Botany* 97: 1732–1748.

Schubert M, Marcussen T, Meseguer AS, Fjellheim S. 2019. The grass subfamily Pooideae: Cretaceous–Palaeocene origin and climate-driven Cenozoic diversification. *Global Ecology and Biogeography* 28: 1168–1182.

Skendzic EM, Columbus JT, Cerros-Tlatilpa R. 2007. Phylogenetics of Andropogoneae (Poaceae: Panicoideae) based on nuclear ribosomal internal transcribed spacer and chloroplast *trnL-F* sequences. *Aliso* 23: 530–544.

Soenarko S. 1977. The genus *Cymbopogon* Sprengel (Gramineae). *Reinwardtia* 9: 225–375.

Soreng RJ, Peterson PM, Romaschenko K, Davidse G, Teisher JK, Clark LG, Barberá P, Gillespie LJ, Zuloaga FO. 2017. A worldwide phylogenetic classification of the Poaceae (Gramineae) II: An update and a comparison of two 2015 classifications. *Journal of Systematics and Evolution* 55: 259–290.

Sparks AN. 1979. A review of the biology of the fall armyworm. *The Florida Entomologist* 62: 82–87.

Stamatakis A. 2014. RAxML version 8: A tool for phylogenetic analysis and post-analysis of large phylogenies. *Bioinformatics* 30: 1312–1313.

Stapf O. 1917. Gramineae. In: Prain D ed. *Flora of Tropical Africa*, 9, Part 1. London: L. Reeve & Co. 1–192.

Sun Q, Lin Q, Yi Z-L, Yang Z-R, Zhou F-S. 2010. A taxonomic revision of *Miscanthus s.l.* (Poaceae) from China. *Botanical Journal of the Linnean Society* 164: 178–220.

Sundberg MD, Orr AR. 1990. Inflorescence development in two annual teosintes: *Zea mays* subsp. *mexicana* and *Z. mays* subsp. *parviglumis*. *American Journal of Botany* 77: 141–152.

Sur PR. 2001. A revision of the genus *Ischaemum* Linn. (Poaceae) in India. *Journal of Economic and Taxonomic Botany* 25: 407–438.

Talavera G, Castresana J. 2007. Improvement of phylogenies after removing divergent and ambiguously aligned blocks from protein sequence alignments. *Systematic Biology* 56: 564–577.

Teerawatananon A, Jacobs SWL, Hodkinson TR. 2011. Phylogenetics of Panicoideae (Poaceae) based on chloroplast and nuclear DNA sequences. *Telopea* 13: 115–142.

Thompson EJ. 2019. A re-evaluation of the taxonomic status of the Australian species of *Arthraxon* Beauv. and *Thelepogon* Roth (Poaceae: Panicoideae: Andropogoneae). *Austrobaileya* 10: 480–505.

Tian X, Knapp AD, Moore KJ, Brummer EC, Bailey TB. 2002. Cupule removal and caryopsis scarification improves germination of eastern gamagrass seed. *Crop Science* 42: 185–189.

Ueno O. 1995. Occurrence of distinctive cells in leaves of $C_4$ species in *Arthraxon* and *Microstegium* (Andropogoneae-Poaceae) and the structural and immunocytochemical characterization of these cells. *International Journal of Plant Sciences* 156: 270–289.

van den Heuvel E, Veldkamp JF. 2000. Revision of *Hemarthria*. *Blumea* 45: 443–475.

van Welzen PC. 1981. A taxonomic revision of the genus *Arthraxon* Beauv. (Gramineae). *Blumea* 27: 255–300.

Veldkamp JF. 1999. A revision of *Chrysopogon* Trin. including *Vetiveria* Bory (Poaceae) in Thailand and Malesia with notes on some other species from Africa and Australia. *Austrobaileya* 5: 503–533.

Veldkamp JF. 2016a. A revision of *Dimeria* (Gramineae-Dimeriinae) in Malesia with a note on *Cymbachne*. *Blumea* 61: 207–214.

Veldkamp JF. 2016b. A revision of *Themeda* (Gramineae) in Malesia with a new species from Laos. *Blumea* 61: 29–40.

Veldkamp JF, de Koning R, Sosef MSM. 1986. Generic delimitation of *Rottboellia* and related genera (Gramineae). *Blumea* 31: 281–307.

Vicentini A, Barber JC, Aliscioni SS, Giussani LM, Kellogg EA. 2008. The age of the grasses and clusters of origins of $C_4$ photosynthesis. *Global Change Biology* 14: 2963–2977.

Vorontsova MS, Besnard G, Razanatsoa J, Hackel J. 2020. The endemic 'sugar canes' of Madagascar (Poaceae, Saccharinae: *Lasiorhachis*) are close relatives of sorghum. *Botanical Journal of the Linnean Society* 192: 148–164.

Vorontsova MS, Ratovonirina G, Randriamboavonjy T. 2013. Revision of *Andropogon* and *Diectomis* (Poaceae: Sacchareae) in

Madagascar and the new *Andropogon itremoensis* from the Itremo Massif. *Kew Bulletin* 68: 193–207.

Watson L, Dallwitz MJ. 1992. *The grass genera of the world*. Wallingford: C.A.B. International.

Welker CAD, Kellogg EA, Prado J. 2014. Andropogoneae versus Sacchareae (Poaceae: Panicoideae): The end of a great controversy. *Taxon* 63: 643–646.

Welker CAD, McKain MR, Vorontsova MS, Peichoto MC, Kellogg EA. 2019. Plastome phylogenomics of sugarcane and relatives confirms the segregation of the genus *Tripidium* (Poaceae: Andropogoneae). *Taxon* 68: 246–267.

Welker CAD, Souza-Chies TT, Longhi-Wagner HM, Peichoto MC, McKain MR, Kellogg EA. 2015. Phylogenetic analysis of *Saccharum s.l.* (Poaceae; Andropogoneae), with emphasis on the circumscription of the South American species. *American Journal of Botany* 102: 248–263.

Welker CAD, Souza-Chies TT, Longhi-Wagner HM, Peichoto MC, McKain MR, Kellogg EA. 2016. Multilocus phylogeny and phylogenomics of *Eriochrysis* P. Beauv. (Poaceae–Andropogoneae): Taxonomic implications and evidence of interspecific hybridization. *Molecular Phylogenetics and Evolution* 99: 155–167.

Welker CAD, Souza-Chies TT, Peichoto MC, Oliveira RP, Carvalho LC, Muccillo VBS, Kellogg EA, Kaltchuk-Santos E. 2017. A new allopolyploid species of *Saccharum* (Poaceae—Andropogoneae) from South America, with notes on its cytogenetics. *Systematic Botany* 42: 507–515.

Wu ZY, Raven PH, Hong DY eds. 2006. *Flora of China: Poaceae*. 22. Beijing: Science Press.

Yu Y, Blair C, He X. 2020. RASP 4: Ancestral state reconstruction tool for multiple genes and characters. *Molecular Biology and Evolution* 37: 604–606.

Yu Y, Harris AJ, Blair C, He X. 2015. RASP (reconstruct ancestral state in phylogenies): A tool for historical biogeography. *Molecular Phylogenetics and Evolution* 87: 46–49.

Zuloaga FO, Morrone O, Davidse G, Filgueiras TS, Peterson PM, Soreng RJ, Judziewicz EJ. 2003. Catalogue of new world grasses (Poaceae): III. Subfamilies Panicoideae, Aristidoideae, Arundinoideae and Danthonioideae. *Contributions From the United States National Herbarium* 46: 1–662.

Zuloaga FO, Morrone O, Davidse G, Pennington SJ. 2007. Classification and biogeography of Panicoideae (Poaceae) in the New World. *Aliso* 23: 503–529.

## Supplementary Material

The following supplementary material is available online for this article at http://onlinelibrary.wiley.com/doi/10.1111/jse.12691/suppinfo:

**Table S1.** Voucher specimens, GenBank accession numbers, and origin of the plastome sequences of Andropogoneae and allies included in the present phylogenomic and biogeographic analyses. PI (Plant Introduction) numbers refer to material from USDA-GRIN (United States Department of Agriculture – Germplasm Resources Information Network), and Kew MSB numbers from Millennium Seed Bank (Royal Botanic Gardens, Kew, UK). *Newly assembled from publicly available data.

**Table S2.** Plastome size and assembly statistics representing gaps and coverage (the latter only for new assemblies) of the specimens of Andropogoneae and allies included in the present phylogenomic and biogeographic analyses. LSC (large single-copy region), SSC (small single-copy region), IR (inverted repeats region).

**Table S3.** Number of dispersal events between regions as estimated by the statistical dispersal-vicariance (S-DIVA), dispersal-extinction-cladogenesis (DEC), and Bayesian Binary MCMC (BBM) models based on all possible scenarios at a given node. Area designations are: A = Africa, B = Central America, C = East Asia, D = Europe, E = North America, F = Oceania, G = South America, and H = West Asia.

**Table S4.** Accepted genera of Andropogoneae and their respective subtribes in our classification and in the treatments of Soreng et al. (2017), Kellogg (2015), and Clayton & Renvoize (1986). Subtribal names in parentheses indicate that the respective genus was considered a synonym of another genus from that subtribe in the respective classification. N/A indicates that the genus was not listed in that classification.

**Fig. S1.** Dispersal-extinction-cladogenesis (DEC) biogeographical estimation results for Andropogoneae plus select members of Arundinelleae, Jasenelleae, and Paspaleae displayed on a chronogram reconstructed using complete plastome sequences. Pie charts indicate ancestral area frequencies with areas and corresponding colors in the legend. Ancestral areas with a frequency of less than 25% present in at least one node are colored black and labeled "Other". RASP node numbers are indicated for subtribes and other nodes discussed in the text.

**Fig. S2.** Bayesian Binary MCMC (BBM) biogeographical estimation results for Andropogoneae plus select members of Arundinelleae, Jasenelleae, and Paspaleae displayed on a chronogram reconstructed using complete plastome sequences. Pie charts indicate ancestral area frequencies with areas and corresponding colors in the legend. Ancestral areas with a frequency of less than 25% present in at least one node are colored black and labeled "Other". RASP node numbers are indicated for subtribes and other nodes discussed in the text.

**Appendix I.** A new classification of Andropogoneae is proposed in this paper. Accepted names are highlighted in bold and the main synonymous names of genera are presented in parentheses. The approximate number of species of each genus is shown in square brackets []. Genera not sampled in our present plastome analyses were tentatively placed here based on previously published phylogenetic analyses (marked with one asterisk *) or solely on morphology (marked with two asterisks **).

Tribe **Andropogoneae** Dumort., Observ. Gramin. Belg. 84, 90, 141. 1824. Type: *Andropogon* L., Sp. Pl. 2: 1045. 1753.

The tribe includes 14 subtribes, 92 genera, and ~1224 species. Relationships among the subtribes, based on our plastome phylogeny, are summarized in Fig. 4.

1. Subtribe **Arthraxoninae** Benth., J. Linn. Soc., Bot. 19: 46, 67. 1881. Type: *Arthraxon* P. Beauv., Ess. Agrostogr. 111, pl. 11, f. 6. 1812.
   The subtribe includes one genus and ~27 species:
   ***Arthraxon*** P. Beauv. [27]

2. Subtribe **Tripsacinae** Dumort., Anal. Fam. Pl. 64. 1829. Type: *Tripsacum* L., Syst. Nat. (ed. 10) 2: 1253, 1261, 1379. 1759.
The subtribe includes two genera and ~23 species:
***Tripsacum*** L. [16]
***Zea*** L. (=*Euchlaena* Schrad.) [7]

3. Subtribe **Chionachninae** Clayton, Kew Bull. 35(4): 813. 1981. Type: *Chionachne* R. Br., Pl. Jav. Rar. 15, 18. 1838.
The subtribe includes three genera and ~12 species:
***Chionachne*** R. Br. (=*Sclerachne* R. Br.) [9]
***Polytoca*** R. Br. (=*Cyathorhachis* Nees) [2]
***Trilobachne**** M. Schenck ex Henrard [1]

4. Subtribe **Rhytachninae** Welker & E.A. Kellogg, subtribe nov. Type: *Rhytachne* Desv. ex Ham., Prodr. Pl. Ind. Occid. xiv, 11. 1825.
The subtribe includes five genera and ~26 species:
***Loxodera*** Launert (=*Lepargochloa* Launert) [5]
***Oxyrhachis*** Pilg. [1]
***Rhytachne*** Desv. ex Ham. [12]
***Urelytrum*** Hack. [7]
***Vossia*** Wall. & Griff. [1]

5. Subtribe **Chrysopogoninae** Welker & E.A. Kellogg, subtribe nov. Type: *Chrysopogon* Trin., Fund. Agrost. 187. 1820.
The subtribe includes one genus and ~49 species:
***Chrysopogon*** Trin. (=*Vetiveria* Lem.-Lis.) [49]

6. Subtribe **Rottboelliinae** J. Presl, Reliq. Haenk. 1(4–5): 329. 1830. Type: *Rottboellia* Naezén, Nov. Gram. Gen. 13, 114. 1779.
=Coicinae Rchb. ex Clayton & Renvoize, Kew Bull., Addit. Ser. 13: 372. 1986. Type: *Coix* L., Sp. Pl. 2: 972. 1753.
The subtribe includes three genera and ~13 species:
***Chasmopodium**** Stapf (=*Robynsiochloa* Jacq.-Fél.) [3]
***Coix*** L. [4]
***Rottboellia*** Naezén [6]

7. Subtribe **Ratzeburgiinae** Hook. f., Fl. Brit. India 7: 4. 1896 ("1897"). Type: *Ratzeburgia* Kunth, Révis. Gramin. 2: 487. 1831.
The subtribe includes 11 genera and ~87 species:
***Eremochloa*** Buse [12]
***Glyphochloa*** Clayton [9]
***Hackelochloa*** Kuntze [2]
***Hemarthria*** R. Br. [14]
***Heteropholis**** C.E. Hubb. [6]
***Manisuris**** L. [1]
***Mnesithea*** Kunth (=*Coelorachis* Brongn.) [26]
***Ophiuros**** C.F. Gaertn. [4]
***Ratzeburgia**** Kunth [1]
***Thaumastochloa**** C.E. Hubb. [8]
***Thyrsia*** Stapf [4]

8. Subtribe **Ischaeminae** J. Presl, Reliq. Haenk. 1(4–5): 328. 1830. Type: *Ischaemum* L., Sp. Pl. 2: 1049. 1753.
=Dimeriinae Hack. ex C.E. Hubb., Fam. Fl. Pl., Monocot. 227. 1934. Type: *Dimeria* R. Br., Prodr. 204. 1810.
The subtribe includes four genera and ~152 species:
***Andropterum*** Stapf [1]
***Dimeria*** R. Br. (=*Nanooravia* Kiran Raj & Sivad.) [61]
***Eulaliopsis*** Honda [2]
***Ischaemum*** L. (=*Digastrium* (Hack.) A. Camus) [88]

9. Subtribe **Germainiinae** Clayton, Kew Bull. 27(3): 465. 1972. Type: *Germainia* Balansa & Poitr., Bull. Soc. Hist. Nat. Toulouse 7: 344. 1873.
The subtribe includes five genera and ~44 species:
***Apocopis**** Nees [16]
***Germainia*** Balansa & Poitr. [10]
***Imperata*** Cirillo [13]
***Lophopogon**** Hack. [2]
***Pogonatherum*** P. Beauv. [3]

10. Subtribe **Sorghinae** Bluff, Nees & Schauer ex Clayton & Renvoize, Kew Bull., Addit. Ser. 13: 338. 1986. Type: *Sorghum* Moench, Methodus 207. 1794.
The subtribe includes four genera and ~37 species:
***Cleistachne*** Benth. [1]
***Lasiorhachis*** (Hack.) Stapf [3]
***Sarga*** Ewart [9]
***Sorghum*** Moench (=*Hemisorghum* C.E. Hubb. ex Bor, *Vacoparis* Spangler) [24]

11. Subtribe **Saccharinae** Griseb., Spic. Fl. Rumel. 2: 472. 1846. Type: *Saccharum* L., Sp. Pl. 1: 54. 1753.
The subtribe includes three genera and ~64 species:
***Miscanthus*** Andersson (=*Diandranthus* L. Liu, *Miscanthidium* Stapf, *Narenga* Bor, *Rubimons* B.S. Sun, *Sclerostachya* (Andersson ex Hack.) A. Camus, *Triarrhena* (Maxim.) Nakai) [30]
***Pseudosorghum*** A. Camus [2]
***Saccharum*** L. (=*Erianthus* Michx.) [32]

12. Subtribe **Apludinae** Hook. f., Fl. Brit. India 7: 4. 1896 ("1897"). Type: *Apluda* L., Sp. Pl. 1: 82. 1753.
The subtribe includes seven genera and ~68 species:
***Apluda*** L. [1]
***Asthenochloa**** Buse [1]
***Eulalia*** Kunth [34]
***Homozeugos*** Stapf [6]
***Polytrias*** Hack. [1]
***Sorghastrum*** Nash [21]
***Trachypogon*** Nees [4]

13. Subtribe **Anthistiriinae** J. Presl, Reliq. Haenk. 1(4–5): 347. 1830. Type: *Anthistiria* Naezén, Nov. Gram. Gen. 35. 1779.
The subtribe includes nine genera and ~204 species:
***Bothriochloa*** Kuntze (=*Amphilophis* Nash) [37]
***Capillipedium*** Stapf [18]
***Cymbopogon*** Spreng. [59]
***Dichanthium*** Willemet [22]
***Eremopogon**** Stapf [4]
***Euclasta*** Franch. (=*Indochloa* Bor) [2]
***Heteropogon*** Pers. [6]
***Iseilema*** Andersson [24]
***Themeda*** Forssk. (=*Anthistiria* Naezén) [32]

14. Subtribe **Andropogoninae** J. Presl, Reliq. Haenk. 1(4–5): 331. 1830. Type: *Andropogon* L., Sp. Pl. 2: 1045. 1753.
The subtribe includes 11 genera and ~292 species:
***Anadelphia*** Hack. (=*Monium* Stapf, *Pobeguinea* (Stapf) Jacq.-Fél.) [14]
***Andropogon*** L. (=*Hypogynium* Nees) [125]
***Bhidea***** Stapf ex Bor [3]
***Diectomis*** Kunth [1]
***Diheteropogon*** (Hack.) Stapf [4]
***Elymandra*** Stapf (=*Pleiadelphia* Stapf) [6]
***Exotheca*** Andersson [1]
***Hyparrhenia*** Andersson ex E. Fourn. (=*Dybowskia* Stapf) [58]
***Hyperthelia*** Clayton [7]
***Monocymbium*** Stapf [3]
***Schizachyrium*** Nees (=*Ystia* Compère) [70]

*Incertae sedis*
Twenty-three genera and ~126 species are placed *incertae sedis* in this classification pending additional data.

Position isolated, unresolved, or poorly supported in trees:
***Agenium**** Nees [4]
***Elionurus*** Humb. & Bonpl. ex Willd. [17]
***Eriochrysis*** P. Beauv. (=*Leptosaccharum* (Hack.) A. Camus) [11]
***Jardinea*** Steud. [3]
***Kerriochloa*** C.E. Hubb. [1]
***Lasiurus*** Boiss. [1]
***Leptatherum**** Nees (=*Polliniopsis* Hayata) [3]
***Microstegium*** Nees (=*Ischnochloa* Hook. f.) [27]
***Parahyparrhenia*** A. Camus [6]
***Phacelurus**** Griseb. (=*Pseudovossia* A. Camus) [6]
***Pseudopogonatherum**** A. Camus [5]
***Sehima*** Forssk. [5]
***Spodiopogon**** Trin. (=*Eccoilopus* Steud.) [18]
***Thelepogon*** Roth [2]
***Tripidium*** H. Scholz [6]

No molecular data available and no clear morphological synapomorphies to place in a subtribe:
***Clausospicula***** Lazarides [1]
***Lakshmia***** Veldkamp [1]
***Pogonachne***** Bor [1]
***Pseudanthistiria***** (Hack.) Hook. f. [4]
***Pseudodichanthium***** Bor [1]
***Spathia***** Ewart [1]
***Triplopogon***** Bor [1]
***Veldkampia***** Y. Ibaragi & Shiro Kobay. [1]